Clim. Past Discuss., https://doi.org/10.5194/cp-2017-104
Manuscript under review for journal Clim. Past
Discussion started: 24 August 2017

Climate of the Past Discussions

Holocene aridification trend interrupted by millennial- and centennial-scale climate fluctuations from a new sedimentary record from Padul (Sierra Nevada, southern Iberian Peninsula)

María J. Ramos-Román[1], Gonzalo Jiménez-Moreno[1], Jon Camuera[1], Antonio García-Alix[1], R. Scott Anderson[2], Francisco J. Jiménez-Espejo[3], José S. Carrión[4]

[1] Departamento de Estratigrafía y Paleontología, Universidad de Granada, Spain
[2] School of Earth Sciences and Environmental Sustainability, Northern Arizona University, USA.
[3] Department of Biogeochemistry, Japan Agency for Marine-Earth Science and Technology (JAMSTEC), Japan.
[4] Departamento de Biología Vegetal, Facultad de Biología, Universidad de Murcia, Murcia, Spain.

Correspondence to: María J. Ramos-Román (mjrr@ugr.es)

Abstract. Holocene centennial-scale paleoenvironmental variability has been described in a multiproxy analysis (i.e. lithology, geochemistry, macrofossil and microfossil analyses) of a paleoecological record from the Padul basin in Sierra Nevada, southern Iberian Peninsula. This sequence covers a relevant time interval hitherto unreported in the studies of the Padul sedimentary sequence. The ca. 4700 yr-long record has preserved proxies of climate variability, with vegetation, lake levels and sedimentological change the Holocene in one of the most unique and southernmost peat bogs from Europe. The progressive Middle and Late Holocene trend toward arid conditions identified by numerous authors in the western Mediterranean region, mostly related to a decrease in summer insolation, is also documented in this record, being here also superimposed by centennial-scale variability in humidity. In turn, this record shows centennial-scale climate oscillations in temperature that correlate with well-known climatic events during the Late Holocene in the western Mediterranean region, synchronous with variability in solar and atmospheric dynamics. The multiproxy Padul record first shows a transition from a relatively humid Middle Holocene in the western Mediterranean region to more aridity from ~4700 to ~2800 cal yr BP. A relatively warm and humid period occurred between ~2600 to ~1600 cal yr BP, coinciding with persistent negative NAO conditions and the historic Iberian-Roman Humid Period. Enhanced arid conditions, co-occurring with overall positive NAO conditions and increasing solar activity, are observed between ~1550 to ~ 450 cal yr BP (~400 to ~1400 CE) and colder and warmer conditions happened during the Dark Ages and Medieval Climate Anomaly, respectively. Slightly wetter conditions took place during the end of the MCA and the first part of the Little Ice Age, which could be related to a change towards negative NAO conditions and minima in solar activity. Evidences of higher human impact in the Padul peat bog area are observed in the last ~1550 cal yr BP. Time series analysis performed from local (*Botryococcus* and TOC) and regional signals (Mediterranean forest) helped us determining the relationship between southern Iberian climate evolution, atmospheric, oceanic dynamics and solar activity.

Keywords: Holocene, Padul**,** peat bog, North Atlantic Oscillation, atmospheric dynamics, southern Iberian Peninsula, Sierra Nevada, western Mediterranean.

Clim. Past Discuss., https://doi.org/10.5194/cp-2017-104
Manuscript under review for journal Clim. Past
Discussion started: 24 August 2017

1 Introduction

The Mediterranean area is situated in a sensitive region between temperate and subtropical climates making it an important place to study the connections between atmospheric and oceanic dynamics and environmental changes. Climate in the western Mediterranean and the southern Iberian Peninsula is influenced by several atmospheric and oceanic dynamics (Alpert et al., 2006), including the North Atlantic Oscillation (NAO) one of the principal atmospheric phenomenon controlling climate in the area (Hurrell, 1995; Moreno et al., 2005). Recent NAO reconstructions in the western Mediterranean region relate negative and positive NAO conditions with an increase and decrease in winter (effective) precipitation, respectively (e.g. Olsen et al., 2012; Trouet et al., 2009). Numerous paleoenvironmental studies in the western Mediterranean have detected a link at millennial- and centennial-scales between the oscillations of paleoclimate proxies studied in sedimentary records with solar variability and atmospheric (i.e., NAO) and/or ocean dynamics during the Holocene (e.g. Fletcher et al., 2013; Moreno et al., 2012; Rodrigo-Gámiz et al., 2014). Very few montane and low altitude lake records in southern Iberia document centennial-scale climate change [see, for example Zoñar Lake (Martín-Puertas et al., 2008)], with most terrestrial records in the western Mediterranean region evidencing only millennial-scale cyclical changes. Therefore, higher-resolution decadal-scale analyses are thus necessary in order to analyze the link between solar activity, atmospheric and oceanographic systems with terrestrial environment in this area at shorter (ie., centennial) time scales.

Sediments from lakes, peat bogs and marine records from the western Mediterranean have documented an aridification trend during the Late Holocene (e.g. Carrión et al., 2010b; Gil-Romera et al., 2014; Jalut et al., 2009). This trend, however, was superimposed by shorter-term climate variability, as shown by several recent studies from the region, as well as human pressure (Carrión, 2002; Fletcher et al., 2013; Jiménez-Moreno et al., 2013; Martín-Puertas et al., 2008; Ramos-Román et al., 2016). This relationship between climate variability, culture evolution and human impact during the Late Holocene has also been the subject of recent paleoenvironmental studies (Carrión et al., 2007; Lillios et al., 2016; López-Sáez et al., 2014; Magny, 2004). However, it is still unclear what has been the main forcing driving environmental change (i.e., deforestation) in this area during this time: was it climate or humans?

Within the western Mediterranean region, Sierra Nevada is the highest and southernmost mountain range in the Iberian Peninsula and thus presents a critical area for paleoenvironmental studies. Most high-resolution studies there have come from high elevation sites. The well-known Padul peat bog site is located at the western foot of the Sierra Nevadas (Fig. 1) and bears one of the longest continental records in southern Europe, with a sedimentary sequence of ca. 100 m thick that could represent the last 1 Ma (Ortiz et al., 2004). Several research studies, including radiocarbon dating, geochemistry and pollen analyses, have been carried out on previous cores from Padul, and have documented glacial/interglacial cycles during the Pleistocene and up until the Middle Holocene. However, the Late Holocene section of the Padul sedimentary sequence has never been retrieved and studied. This was due to the location of these previous corings within the peat mine exploitation setting, where the upper (and non productive) part of the sedimentary sequence was missing (Florschütz et al., 1971; Ortiz et al., 2004; Pons and Reille, 1988).

Here we present a new record from the Padul peat bog basin: Padul-15-05, a 42.64 m-long sediment core that, for the first time, contains a continuous record of the Late Holocene (Fig. 2). A high-resolution multi-proxy analysis of the upper 1.15 m, the past ~4700 cal yr BP, has allowed us to determine a complete paleoenvironmental and paleoclimatic record at centennial-

Clim. Past Discuss., https://doi.org/10.5194/cp-2017-104
Manuscript under review for journal Clim. Past
Discussion started: 24 August 2017

and millennial-scales. To accomplish that, we reconstructed changes in the Padul peat bog vegetation, sedimentation, climate and human impact during the Holocene throughout the interpretation of the lithology, palynology and geochemistry.
Specifically, the main objective of this paper is to determine environmental variability and climate evolution in the southern Iberian Peninsula and the western Mediterranean region and their linkages to northern hemisphere climate and solar variability during the Holocene. In order to do this, we compared our results with other paleoclimate records from regional areas and solar activity from the northern hemisphere for the past ca. 4.7 cal ka BP (Bond et al., 2001; Laskar et al., 2004; Sicre et al., 2016; Steinhilber et al., 2009).

2 Study site

2.1 Regional setting: Sierra Nevada climate and vegetation

Sierra Nevada is a W-E aligned mountain range located in Andalusia (southern Spain). Climate in this area is Mediterranean, with cool and humid winters and hot/warm summer drought. In the Sierra Nevada, the mean annual temperature at approximately 2500 m asl is 4.5 ºC and the mean annual precipitation is 700 mm/yr (Oliva et al., 2009). Sierra Nevada is strongly influenced by thermal and precipitation variations due to the altitudinal gradient (from ca. 700 to more than 3400 m), which control plant taxa distribution in different bioclimatic vegetation belts due to the variability in thermotypes and ombrotypes (Valle Tendero, 2004). According to the climatophilous series classification, Sierra Nevada is divided in four different vegetation belts (Fig. 1). The crioromediterranean vegetation belt, occurring above ~2800 m, is characterized principally by *Festuca clementei*, *Hormatophylla purpurea*, *Erigeron frigidus*, *Saxifraga nevadensis*, *Viola crassiuscula*, and *Linaria glacialis*. The oromediterranean belt, between ~1900 to 2800 m, bears *Pinus sylvestris*, *P. nigra*, *Juniperus communis subsp. hemisphaerica*, *J. sabina* var. *humilis*, *J. communis* subsp. *nana*, *Genista versicolor*, *Cytisus oromediterraneus*, *Hormatophylla spinosa*, *Prunus prostrata*, *Deschampsia iberica* and *Astragalus sempervirens* subsp. *nevadensis* as the most representative species. The supramediterranean belt, from approximately 1400 to 1900 m of elevation, principally includes *Quercus pyrenaica*, *Q. faginea*, *Q. rotundifolia*, *Acer opalus* subsp. *granatense*, *Fraxinus angustifolia*, *Sorbus torminalis*, *Adenocarpus decorticans*, *Helleborus foetidus*, *Daphne gnidium*, *Clematis flammula*, *Cistus laurifolius*, *Berberis hispanicus*, *Festuca scariosa, Thymus serpylloides* subsp. *gadoriensis, Helichrysum italicum* subsp. *serotinum*, *Santolina rosmarinifolia* subps. *canescens* and *Artemisia glutinosa*. The mesomediterranean vegetation belt occurs between ~600 and 1400 m of elevation and is characterized by *Quercus rotundifolia*, *Retama sphaerocarpa*, *Paeonia coriacea*, *Juniperus oxycedrus*, *Rubia peregrina*, *Asparagus acutifolius*, *D. gnidium*, *Ulex parviflorus*, *Genista umbellata*, *Cistus albidus* and *C. lauriflolius* (Al Aallali et al., 1998; Valle, 2003). The human impact over this area, especially important during the last millennium, affected the natural vegetation distribution through fire, deforestation, cultivation. (i.e., *Olea*) and subsequent reforestation (mostly *Pinus)* (Anderson et al., 2011).

2.2 Padul peat bog

The Padul basin is situated at approximately 725 m of elevation in the southeastern part of the Granada Basin, at the foothill of the southwestern Sierra Nevada, Andalucía, Spain (Fig. 1). This is one of the most seismically active areas in the southern Iberian Peninsula with numerous faults

Clim. Past Discuss., https://doi.org/10.5194/cp-2017-104
Manuscript under review for journal Clim. Past
Discussion started: 24 August 2017

Climate of the Past Discussions

in NW-SE direction, with the Padul fault being one of these active normal faults (Alfaro et al., 2001). It is a small extensional basin approximately 12 km long and covering an area of approximately 45 km^2, which is bounded by the Padul normal fault. The sedimentary in-filling of the basin consists of Neogene and Quaternary deposits; Upper Miocene conglomerates, calcarenites and marls, and Pliocene and Quaternary alluvial sediments, lacustrine and peat bog deposits (Sanz de Galdeano et al., 1998; Delgado et al., 2002; Domingo et al., 1983). The Padul peat bog is an endorheic area with a surface of approximately 4 km^2 placed in the Padul basin that contains a sedimentary sequence mostly characterized by peat. The basin fill is asymmetric, with thicker peat infill to the northeast (~100 m thick; Domingo-García et al., 1983; Florschütz et al., 1971; Nestares and Torres, 1997) and disappearing to the southwest (Alfaro et al., 2001). The main source area of the sediments in the Padul peat bog is Sierra Nevada, which is characterized at higher elevations by Paleozoic siliceous metamorphic rocks (mostly mica-schists and quartzites) from the Nevado-Filabride complex and, at lower elevations and acting as bedrock, by Triassic dolomites, limestones and phyllites from the Alpujárride Complex (Sanz de Galdeano et al. 1998). Geochemistry in the Padul sediments is influenced by detritic materials coming from the neighboring mountains, mainly the Sierra Nevada mountain range (Ortiz et al., 2004). In addition, groundwater inputs into the Padul basin are the main reason why there is a wetland in this area. These inputs come from the Triasic carbonates aquifers (N and S edge to the basin), the out flow of the Granada Basin (W) and the conglomerate aquifer to the east edge (Castillo Martín et al., 1984; Ortiz et al., 2004). The main water output is by evaporation and evapotranspiration, water wells and by canals ("madres") that drain the water to the Dúrcal river to the southeast (Castillo Martín et al., 1984). Climate in the Padul area is characterized by a mean annual temperature of 14.4 ºC and a mean annual precipitation of 445 mm (http://www.aemet.es/).

Vegetation in the Padul area is dominated by *Q. rotundifolia* (and in less amounts *Q. faginea*), which is normally accompanied by *Pistacia terebinthus*. Shrub species in the area include *Juniperus oxycedrus*, *Crataegus monogyna*, *Daphne gnidium* and *Ruscus aculeatus*. Creepers such as *Lonicera implexa*, *Rubia peregrina*, *Hedera helix*, *Asparagus acutifolius* also occur in this area and some herbs, such as *Paeonia broteroi*. *Quercus coccifera* also occurs in crests and very sunny rocky outcrops. *Retama sphaerocarpa* and *Genista cinerea* subsp. *speciosa* and the *Thymo-Stipetum tenacissime* series also occur in sunny areas and in more xeric soils. Nitrophilous communities occur in soils disrupted by livestock, pathways or open forest, normally related with anthropization (Valle, 2003).

The Padul-15-05 drilling site was located around 50 m south of the present-day Padul lake shore area. This basin area is presently subjected to seasonal water level fluctuations and is principally dominated by *Phragmites australis* (Poaceae). The lake environment is dominated by aquatic and wetland communities with *Chara vulgaris*, *Myriophyllum spicatum, Potamogeton pectinatus, Potamogetum coloratus*, *Phragmites australis, Typha dominguensis*, *Apium nodiflorum*, *Juncus subnodulosus, Carex hispida*, *Juncus bufonius and Ranunculus muricatus* between others (Pérez Raya and López Nieto, 1991). Some sparse riparian trees occur in the northern lake shore, such as *Populus alba*, *Populus nigra*, *Salix* sp., *Ulmus minor* and *Tamarix*.

3 Material and methods

Two sediment cores, Padul-13-01 (37º00'40''N; 3º36'13''W) and Padul-15-05 (37º00'39.77''N; 3º36'14.06''W) with a length of 58.7 cm and 42.64 m, respectively, were collected between 2013 and 2015 from the peat bog (Fig. 1). The cores were taken using a Rolatec RL-48-L drilling

Clim. Past Discuss., https://doi.org/10.5194/cp-2017-104
Manuscript under review for journal Clim. Past
Discussion started: 24 August 2017

machine equipped with a hydraulic piston corer from the Scientific Instrumentation Centre of the University of Granada. The sediment cores were wrapped in film, put in core boxes, transported and stored in a dark cool room at +4ºC.

3.1 Age-depth model (AMS radiocarbon dating)

The core chronology was constrained using fourteen AMS radiocarbon dates from plant remains and organic bulk samples taken throughout the cores (Table 1). In addition, one sample with gastropods was also measured for AMS radiocarbon analysis, although it was rejected due to important reservoir effect, which provide a very old date. Thirteen of these samples came from Padul-15-05 and one from the nearby Padul-13-01 (Table 1). We were able to use this date from Padul-13-01 core as there is a very significant correlation between the upper part of Padul-15-05 and Padul-13-01 cores, shown by identical lithological and geochemical changes (Supplementary information 1; Figure S1). The age model for the upper ~3 m until 21 cm from the surface was built using the R-code package 'Clam 2.2' (Blaauw, 2010) employing the calibration curve IntCal 13 (Reimer et al., 2013), a 95 % of confidence range, a smooth spline (type 4) with a 0.20 smoothing value and 1000 iterations (Fig. 2). The chronology of the uppermost 21 cm of the record was built using a lineal interpolation between the last radiocarbon date and the top of the record (Present; 2015 CE). The studied interval in the present work are the uppermost 115 cm of the record that are constrained by six AMS radiocarbon dates (Fig. 2).

3.2 Lithology, MS, XRF and TOC

The length for the Padul-15-05 core is ~ 43 m. In this study, we focus in the uppermost ~ 115 cm from that core. Padul-15-05 core was split longitudinally and was described in the laboratory with respect to lithology and color (Fig. 3).

Magnetic susceptibility (MS) was measured with a Bartington MS3 operating with a MS2E sensor. MS measurements (in SI units) were obtained directly from the core surface every 0.5 cm (Fig. 3).

Elemental geochemical composition was measured in an X-Ray fluorescence (XRF) Avaatech core scanner® at the University of Barcelona (Spain). A total of thirty-three chemical elements were measured in the XRF core scanner at 10 mm of spatial resolution, using 10 s count time, 10 kV X-ray voltage and a X-ray current of 650 μA for lighter elements and 35 s count time, 30 kV X-ray voltage, X-ray current of 1700 μA for heavier elements. Thirty-three chemical elements were measured but only the most representative with a major number of counts were considered (Si, K, Ca, Ti, Fe, Zr, Br and Sr). Results for each element are expressed as intensities in counts per second (cps) and normalized (norm.) for the total sum in cps in every measure (Fig. 3).

Total organic carbon (TOC) was analyzed every 2 or 3 cm throughout the core. Samples were previously decalcified with 1:1 HCl in order to eliminate the carbonate fraction. The percentage of organic Carbon (OC %) was measured in an Elemental Analyzer Thermo Scientific Flash 2000 model from the Scientific Instrumentation Centre of the University of Granada (Spain). Percentage of TOC per gram of sediment was calculated from the percentage of organic carbon (OC %) yielded by the elemental analyzer, and recalculated by the weight of the sample prior to decalcification (Fig. 3).

3.3 Pollen and NPP

Clim. Past Discuss., https://doi.org/10.5194/cp-2017-104
Manuscript under review for journal Clim. Past
Discussion started: 24 August 2017

Samples for pollen analysis (1-3 cm^3) were taken every 1 cm throughout the core. Pollen extraction methods followed a modified Faegri and Iversen (1989) methodology. Processing included the addition of *Lycopodium* spores for calculation of pollen concentration. Sediment was treated with NaOH, HCl, HF and the residue was sieved at 250 mm previous to an acetolysis solution. Counting was performed using a transmitted light microscope at 400 magnifications to an average pollen count of ca. 260 terrestrial pollen grains. Fossil pollen was identified using published keys (Beug, 1961) and modern reference collections at University of Granada (Spain). Pollen counts were transformed to pollen percentages based on the terrestrial pollen sum, excluding aquatics. The palynological zonation was executed by cluster analysis using twelve different pollen taxa- *Olea*, *Pinus* undifferentiated, deciduous *Quercus*, evergreen *Quercus*, *Pistacia*, Ericaceae, *Artemisia*, Asteroideae, Cichorioideae, Amaranthaceae and Poaceae (Grimm, 1987) (Fig. 4). Non-pollen palynomorphs (NPP) include fungal and algal spores, and thecamoebians (testate amoebae). The NPP percentages were calculated and represented with respect to the terrestrial pollen sum (Fig. 4). Furthermore, some pollen taxa were grouped, according to present-day ecological bases, in Mediterranean forest and xerophytes (Fig. 4). The Mediterranean forest taxa is composed of *Quercus* total, *Olea*, *Phillyrea* and *Pistacia*. The xerophyte group includes *Artemisia*, *Ephedra*, and Amaranthaceae.

4 Results

4.1 Chronology and sedimentation rates

The age-model of the studied Padul-15-05 core (Fig. 2) shows that the top 115 cm continuously cover approximately the last ca. 4700 cal yr BP, being the age constrained by fourteen AMS ^{14}C dates (Table 1). Five distinct sediment accumulation rate (SAR) intervals can be differentiated between 0 and 122.96 cm based on the linear interpolation between radiocarbon dates in the studied core (Fig. 2).

4.2 Lithology, MS, XRF and TOC

The lithology of the upper ca. 115 cm of the Padul-15-05 sediment core was mainly deduced from a visual inspection together with the element geochemical composition (XRF) and the correlation of these data, and the MS of the split cores. In addition, this information was complemented with the TOC (Fig. 3).
A Linear r (Pearson) correlation was calculated for the XRF data, the correlation for the inorganic geochemical elements show us two different groups of elements that covary (Table 2): Group 1) Si, K, Ti, Fe and Zr with a high positive correlation between them; Group 2) Ca, Br and Sr have negative correlation with Group 1. The lithology for this sedimentary sequence consists in clays with variable carbonates, siliciclastics and organic content (Fig. 3). Based on this, the sequence is subdivided in two principal sedimentary units. The bottom of the record corresponds with Unit 1, characterized principally by lower values of MS and higher values of Ca. The top of the sequence can be subdivided in Unit 2, in which the mineralogical composition is lower in Ca with higher values of MS in correlation with mostly siliciclastics elements (Si, K, Ti, Fe and Zr). Within these two units, four different facies can be identified by visual inspection and by the elemental geochemical composition and TOC of the sediments. *Facies* 1, between 115-110 cm depth (ca. 4700 to 4650 cal yr BP) and 89-80 cm depth (ca. 4300 to 4000 cal yr BP), are characterized by dark brown organic clays that bear charophytes and plant remains. They are

Clim. Past Discuss., https://doi.org/10.5194/cp-2017-104
Manuscript under review for journal Clim. Past
Discussion started: 24 August 2017

also depicted by relative higher values of TOC values (Fig. 3). *Facies* 2, between 110-89 cm depth (ca. 4650 to 4300 cal yr BP) and 80-42 cm depth (ca. 4000 to 1600 cal yr BP), are made up of brown clays, with the occurrence of gastropods and charophytes. These are also characterized with decreasing TOC values. *Facies* 3, between 42-28 cm depth (ca. 1600 to 450 cal yr BP), are characterized by grayish brown clays with the occurrence of gastropods, and lower values of TOC, the increasing trend in MS and in siliciclastic elements. *Facies* 4, between 28-0 cm/ ca. 450 cal yr BP to Present, are made up of light grayish brown clays and feature a strong increase in siliciclastic linked to a strong increase in MS.

4.3 Pollen and NPP

A total of seventy-two pollen taxa were identified but only the most representative taxa are here plotted in a summary pollen diagram (Fig. 4). Selected NPP percentages are also displayed in Figure 4. Four pollen zones (Fig. 4) were visually identified with the help of a cluster analysis using the program CONISS (Grimm, 1987). Pollen zones are described below:

4.3.1 Zone Padul-15-05-1 [~4720 to 3400 cal yr BP/ ~2800 to 1450 BCE (115-65 cm)]

Zone 1 is characterized by the abundance of Mediterranean forest species reaching up to ca. 70 %. Another important taxon in this zone is *Pinus,* with average values around 18 %. Herbs are largely represented by Poaceae, averaging around 10 %, and reaching up to ca. 25 %. This pollen zone is subdivided into subzones-1a, 1b and 1c (Fig. 4). The principal characteristic that differentiate subzone-1a to subzone-1b (boundary at ca. 4650 cal yr BP/ca. 2700 BCE) is the decrease in Poaceae from an average value of ca. 18 to 10 %, the increase in *Pinus* from ca. 7 to 18 %, and the appearance of cf. *Vitis.* The decrease in Mediterranean forest to average values around 40 %, the increase in *Pinus* to average values around 25 % and a progressive increase in Ericaceae with average occurrences from ca. 6 to 11 %, allow to discern subzones 1b and 1c (boundary at ca. 3950 cal yr BP).

4.3.2. Zone Padul-15-05-2 [~3400 to 1550 cal yr BP/~1450 BCE to 400 CE (65-41 cm)]

The main features of this zone are the increase in Ericaceae up to ca. 16 % and in deciduous *Quercus*, reaching values around 20 %. Therefore, the Mediterranean forest component progressively decreased to values around 34 %. Some herbs such as Cichorioideae became more abundant reaching average occurrences around 7 %. This pollen zone can be subdivided in subzones 2a and 2b with a boundary at ~2850 cal yr BP (~900 BCE). The principal characteristics that differentiate these subzones is marked by the increase in Mediterranean forest types and the increasing trend in deciduous *Quercus* and Ericaceae. The increase in *Botryococcus* averages ca. 4 to 9 % and the expansion of *Mougeotia and Zygnema* type are also noticeable.

4.3.3 Zone Padul-15-05-3 [~1550 to 450 cal yr BP/~400 CE to 1500 CE (41-29 cm)]

This zone is distinguished by the maximum depletion of Mediterranean forest elements. Cichorioideae reached average values of about 40 %. The decrease in Ericaceae is also significant. A decrease in *Botryococcus* and other algal remains is observed in this zone, although there is an increase in other Thecamoebians from average values <1 % to 10 %. This pollen zone is subdivided in subzones 3a and 3b at ~1000 cal yr BP (~950 CE). The main

Clim. Past Discuss., https://doi.org/10.5194/cp-2017-104
Manuscript under review for journal Clim. Past
Discussion started: 24 August 2017

features that differentiate these subzones are the increase in *Olea* from subzone 3a to 3b from average values of ca. 1 to 5 %. The increasing trend in Poaceae is also a feature in this subzone, as well as the slight increase in Asteroideae at the top. Significant changes are documented in NPP percentages in this subzone with the expansion of some fungal remain such as *Tilletia* and *Glomus* type. Furthermore, a decrease in *Botrycoccus* and the near disappearance of other algal remains such as *Mougetia* occurred.

4.3.4 Zone Padul-15-05-4 [~last 450 cal yr BP/ ~ 1500 CE to Present (29-0 cm)]

The main feature in this zone is the significant increase in *Pinus,* reaching maximum values (ca. 32 %), an increase in Poaceae (ca. 40 %) and the decrease in Cichorioideae (from average occurrences of ca. 44 to 16 %). Other important changes are the nearly total disappearance of some shrubs such as *Pistacia* and a decreasing trend in Ericaceae, as well as an important decrease in Mediterranean forest pollen. An increase in wetland pollen taxa, mostly *Typha* also occurred. A significant increase in xerophytes, with the expansion of Amaranthaceae to ~14 %, is also observed in this period. Other herbs such as *Plantago*, Polygonaceae and Convolvulaceae show moderate increases. This zone 4 is subdivided into subzones 4a and 4b (Fig. 4). The top of the record, which corresponds approximately 1830 CE to Present, is characterized by the subzone 4b, the main characteristic that differentiate subzone 4b from the previous 4a is a decrease in some herbs such as Cichorioideae. However, an increase in some xerophytic herbs such as Amaranthaceae occurred. The increase in *Plantago* is also significant during this period. A noteworthy increase in *Pinus* (from an average of ca. 14 to 27 %) and a slight increase in *Olea* and evergreen *Quercus* are also characteristic of this subzone. With respect to NPP, there is an increase in thecamoebians such as *Arcella* type and in the largely coprophilous sordariaceous (Sordariales) group. This zone also documents the decrease in fresh-water algal spores, in *Botryococcus* concomitant with *Mougeotia and Zygnema type*.

4.4 Estimated lake level reconstruction

Different local proxies from the Padul-15-05 record [Si, Ca, TOC, MS, Hygrophytes (made up of Cyperaceae and Typha), Poaceae and Algae (including Botryoccocus, Zygnema type and Mougeotia) groups] have been depicted in order to understand the relationship between lithological, geochemical, and palynological variability and the water lake level oscillations. Sediments with higher values of TOC (more algae and hygrophytes), rich in Ca (related with the occurrence of shells and charophytes remains) most likely characterized a shallow water environment. The absence of aquatic shells, decreasing Ca and a lower TOC and/or a higher input of clastic material (higher MS and Si values) into the lake, could be related with lake level lowering, and a shallower wetland environment (increase in Poaceae) (Fig. 5).

4.5 Spectral analysis

Spectral analysis was performed on selected pollen and NPP time series (Mediterranean forest and *Botryococcus)*, as well as TOC in order to identify millennial- and centennial-scale periodicities in the Padul-15-05 record. The mean sampling resolution for pollen and NPP is ca. 50 yr and for geochemical data is ca. 80 yr. Statistically significant cycles, above the 90, 95 and 99 % of confident levels, were found around 800, 680, 300, 240, 200, 170 (Fig. 7).

Clim. Past Discuss., https://doi.org/10.5194/cp-2017-104
Manuscript under review for journal Clim. Past
Discussion started: 24 August 2017

5 Discussion

Different proxies have been used in this study to interpret the paleoenvironmental and hydrodynamic changes recorded in the Padul peat bog sedimentary record during the last 4700 cal yr BP. Palynological analysis (pollen and NPP) is commonly used as a proxy for climate change, lake level variations and human impact and land uses (e.g. Faegri and Iversen, 1990; van Geel et al., 1983). In this study, we used the variations between Mediterranean forest taxa, xerophytes and algal communities for paleoclimatic variability and the occurrence of nitrophilous and ruderal plant communities and some NPPs for identifying human influence in the study area (Fig. 4). Variations in arboreal pollen (AP, including Mediterranean tree species) have previously been used in the Sierra Nevada records as a proxy for humidity changes (Jiménez-Moreno and Anderson, 2012; Ramos-Román et al., 2016). The abundance of the Mediterranean forest has been used as a proxy for climate change in other studies in the western Mediterranean region, with higher forest development generally meaning higher humidity (Fletcher et al., 2013; Fletcher and Sánchez-Goñi, 2008). On the other hand, increases in xerophyte pollen taxa (i.e., *Artemisia*, *Ephedra*, Amaranthaceae) have been used as an indication of aridity in this area (Anderson et al., 2011; Carrión et al., 2007).

The chlorophyceae alga *Botryococcus* sp. has been described as an indicator of freshwater environments, in relatively productive fens, temporary pools, ponds or lakes (Guy-Ohlson, 1992). The high visual and statistical correlation between *Botryococcus* from Padul-15-05 and North Atlantic temperature estimations (Bond et al., 2001; r = -0.63; $p < 0.0001$; between ca. 4700 to 1500 cal ka BP – the decreasing and very low *Botryococcus* occurrence in the last 1500 cal yr BP makes this correlation moderate: r=-0.48; $p < 0.0001$ between 4700 and -65 cal yr BP) seems to show that in this case *Botryococcus* is driven by temperature change and would reflect variations in lake productivity (increasing with warmer water temperatures).

In addition to the palynological analysis, variations in the lithology, geochemistry and macrofossil remains (gastropod shells and charophytes) from the Padul-15-05 core helped us reconstruct the estimated lake level and the local environment changes in the Padul peat bog. Several previous studies on Late Holocene lake records from the Iberian Peninsula show that lithological changes can be used as a proxy for lake level reconstruction (Martín-Puertas et al., 2011; Morellón et al., 2009; Riera et al., 2004). For example, carbonate sediments formed by biogenic remains of gastropods and charophytes are indicative of shallow lake waters (Riera et al., 2004). Furthermore, van Geel et al. (1983), described occurrences of *Mougeotia* and *Zygnema* type (Zygnemataceae) as typical of shallow water environments. The increase in organic matter accumulation deduced by TOC (and Br) could be considered as characteristic of high productivity (Kalugin et al., 2007) in these shallow water environments. On the other hand, increases in clastic input in lake sediments have been interpreted as due to lowering of lake level and more influence of terrestrial-fluvial deposition in a very shallow/ephemeral lake (Martín-Puertas et al., 2008). We used the variations between those proxies to estimate water level (Fig. 5).

Nitrophilous and ruderal pollen taxa (*Convolvulus*, *Plantago lanceolata* type, Urticaceae type and/or *Polygonum avicularis* type) are also very useful as proxies for human impact (Riera et al., 2004). Some species of Cichorioideae have also been described in different studies from the Iberian Peninsula as nitrophilous taxa (Abel-Schaad and López-Sáez, 2013). At the same time, NPP taxa such as some coprophilous fungi, Sordariales and thecamoebians are also used as indicators of anthropization and land use (Carrión et al., 2007; Ejarque et al., 2015; van Geel et al., 1989; Riera et al., 2006). *Tilletia* a grass-parasitizing fungi has been described as an indicator

of grass cultivation in other Iberian records (Carrión et al., 2001b). In this study we also used the NPP mycorrhizal fungus *Glomus* sp. as a proxy for erosive activity. This interpretation comes from a study from van Geel et al. (1989), who correlated erosive events with elevated percentages of *Glomus* cf. *fasciculatum*.

5.1 Late Holocene aridification trend

This study shows that a progressive aridification trend occurred during at least the last ca. 4700 cal yr BP in the southern Iberian Peninsula. The increase in aridity is shown in the Padul-15-05 core by a progressive decrease in Mediterranean forest component and the increase in herbs (Figs. 4 and 7). Lake level interpretations from our record agree with the pollen and show an overall decrease during the Late Holocene, from a shallow water table containing relatively abundant organic matter (high TOC, indicating higher productivity), gastropods and charophytes (high Ca values) to a low-productive ephemeral/emerged environment (high clastic input and MS and decrease in Ca) (Fig. 5). This progressive aridification confirmed by the increase in siliciclastics pointing to a change towards ephemeral (even emerged) environments became more prominent since the last ca. 1550 cal yr BP and then enhanced again in the last 300 cal yr BP to Present. *Glomus*, a spore from mycorrhizal fungi that occur in soils (van Geel et al., 1989), follows a similar pattern of change, which probably points to enhanced soil erosion in the catchment area during the last 1550 cal yr BP. Furthermore, the increase in some proxies indicating human land use during this last period suggests that humans were more active in this area since then.

These results are supported by previous studies from the Mediterranean area using different proxies documenting an aridification trend since the Middle Holocene (Carrión, 2002; Carrión et al., 2010a; Fletcher et al., 2013; Fletcher and Sánchez-Goñi, 2008; Jiménez-Espejo et al., 2014; Jiménez-Moreno et al., 2015). In the western Mediterranean region this decline in forest development during the Middle and Late Holocene is related with a decrease in summer insolation (Fletcher et al., 2013; Jiménez-Moreno and Anderson, 2012). This would produce a progressive cooling, with a reduction in the length of the growing season as well as a decrease in the sea-surface temperature (Marchal et al., 2002), generating a decrease in the land-sea contrast that would be reflected in a reduction of the wind system and a reduced precipitation gradient from sea to shore during the fall-winter season. Also, a reorganization of the general atmospheric circulation with a northward shift of the westerlies - a long-term enhanced positive NAO trend - has been interpreted, inducing drier conditions in this area since 6000 cal yr BP (Magny et al., 2012). The aridification trend can clearly be seen in the nearby alpine records from the Sierra Nevada, where there was little influence by human activity (Anderson et al., 2011; Jiménez-Moreno et al., 2013; Jiménez-Moreno and Anderson, 2012; Ramos-Román et al., 2016).

5.2 Millennial- and centennial-scale climate variability in the Padul peat bog during the Late Holocene

The multi-proxy paleoclimate record from Padul-15-05 shows an overall aridification trend. However, this trend seems to be modulated by millennial- and centennial-scale climatic variability.

5.2.1 Aridity pulses around 4200 (4500, 4300 and 4000 cal yr BP) and around 3000 cal yr BP (3300 and 2800 cal yr BP)

Clim. Past Discuss., https://doi.org/10.5194/cp-2017-104
Manuscript under review for journal Clim. Past
Discussion started: 24 August 2017

Marked aridity pulses are registered in the Padul-15-05 record around 4200 and 3000 cal yr BP (Unit 1; Pollen zones 1 an 2a; Figs. 6 and 7). These arid pulses are mostly evidenced in this record by declines in Mediterranean forest taxa, as well as lake level drops and/or cooling evidenced by a decrease in organic component as TOC and the decrease in *Botryococcus* algae. However, a discrepancy between the local and regional occurs between 3000-2800 cal yr BP, with an increase in the estimated lake level and a decrease in the Mediterranean forest during the late Bronze Age until the early Iron Age (Figs. 6 and 7). The disagreement could be due to deforestation by humans during a very active period of mining in the area observed as a peak in lead pollution in the alpine records from Sierra Nevada (García-Alix et al., 2013) . The aridity pulses agree regionally with recent studies carried out at higher in elevation in the Sierra Nevada, a decrease in AP percentage in Borreguil de la Caldera record around 4000-3500 cal yr BP (Ramos-Román et al., 2016), high percentage of non-arboreal pollen around 3400 cal ka BP in Zoñar lake [Southern Córdoba Natural Reserve; (Martín-Puertas et al., 2008)], and lake desiccation at ca. 4100 and 2900 cal yr BP in Lake Siles (Carrión et al., 2007). Jalut et al. (2009) compared paleoclimatic records from different lakes in the western Mediterranean region and also suggested a dry phase between 4300 to 3400 cal yr BP, synchronous with this aridification phase. Furthermore, in the eastern Mediterranean basin other pollen studies show a decrease in arboreal pollen concentration toward more open landscapes around 3.7 ka cal BP (Magri, 1999). Significant climatic changes also occurred in the Northern Hemisphere at those times and polar cooling and tropical aridity are observed at ca. 4200-3800 and 3500-2500 cal yr BP; (Mayewski et al., 2004), cold events in the North Atlantic [cold event 3 and 2; (Bond et al., 2001)], decrease in solar irradiance (Steinhilber et al., 2009) and humidity decreases in the eastern Mediterranean area at 4200 cal yr BP (Bar-Matthews et al., 2003) that could be related with global scale climate variability (Fig. 6). These generally dry phases between 4.5 and 2.8 in Padul-15-05 are generally in agreement with persistent positive NAO conditions during this time (Olsen et al., 2012).
The high-resolution Padul-15-05 record shows that climatic crises such as the one occurred at ca. 4200 cal yr BP, which seems to be recorded worldwide (Booth et al., 2005), are the product of the sum of more than one single climatic event (i.e., ca. 4500, 4300, 4000 cal yr BP) and thus are affected by climatic variability at centennial-scales.

5.2.2 Iberian-Roman Humid Period (~2600 to 1600 cal yr BP)

High relative humidity is recorded in the Padul-15-05 record between ca. 2600 and 1600 cal yr BP, synchronous with the well-known Iberian-Roman Humid Period (IRHP; between 2600 and 1600 cal yr BP; (Martín-Puertas et al., 2009). This is interpreted in our record due to an increase in the Mediterranean forest species at that time (Unit 1; Pollen Zone 2.b; Figs. 6 and 7). In addition, there is a simultaneous increase in *Botryococcus* algae, which is probably related to higher productivity during warmer conditions. Evidence of a wetter climate around this period has also been shown in other regional records and several alpine records from Sierra Nevada. For example, Jiménez-Moreno et al. (2013) studying a sediment record from the Laguna de la Mula, showed an increase in deciduous *Quercus* in correlation with the maximum in algae between 2500 to 1850 cal yr BP, also evidencing the most humid period of the Late Holocene. A geochemical study from the Laguna de Río Seco (also in Sierra Nevada) also evidenced humid conditions around 2200 cal yr BP by the decrease in Saharan dust input and the increase in detritic sedimentation into the lake suggesting higher rainfall (Jiménez-Espejo et al., 2014). In addition, Ramos-Román et al. (2016) showed an increase in AP in the Borreguil de la Caldera record around 2200 cal yr BP, suggesting an increase in humidity at that time.

Clim. Past Discuss., https://doi.org/10.5194/cp-2017-104
Manuscript under review for journal Clim. Past
Discussion started: 24 August 2017

Other records from the Iberian Peninsula also show this pattern to wetter conditions during the IRHP. For example, high lake levels are recorded in Zoñar Lake in southern Spain between 2460 to 1600 cal yr BP, only interrupted by a relatively arid pulse between 2140 and 1800 cal yr BP (Martín-Puertas et al., 2009). An increase in rainfall is described in the central region of the Iberian Peninsula in a study from the Tablas de Daimiel National Park between 2100 and 1680 cal yr BP (Gil García et al., 2007). Deeper lake levels at around 2650 to 1580 cal yr BP, also interrupted by an short arid event at ca. 2125-1790 cal yr BP, were observed to the north, in the Iberian Range (Currás et al., 2012). The fact that the Padul-15-05 record also shows a relatively arid-cold event between 2150-2050 cal yr BP, just in the middle of this relative humid-warm period, seems to point to a common feature of centennial-scale climatic variability in many western Mediterranean and North Atlantic records (Fig. 6). Humid climate conditions at around 2500 cal yr BP are also interpreted in previous studies from lake level reconstructions from Central Europe (Magny, 2004). Increases in temperate deciduous forest are also observed in marine records from the Alboran Sea around 2600 to 2300 cal yr BP, also pointing to high relative humidity (Combourieu Nebout et al., 2009; Fletcher et al., 2007). Overall humid conditions between 2600 and 1600 cal yr BP seem to agree with predominant negative NAO reconstructions at that time, which would translate into greater winter (and thus more effective) precipitation in the area triggering more development of forest species in the area.
Generally warm conditions are interpreted between 1900 and 1700 cal yr BP in the Mediterranean Sea, with high sea surface temperatures (SSTs), and in the North Atlantic area, with the decrease in Drift Ice Index. In addition, persistent positive solar irradiance occurred at that time. The increase in *Botryococcus* algae reaching maxima during the IRHP also seems to point to very productive and perhaps warmer conditions in the Padul peat bog area (Fig. 6).

5.2.3 DA and MCA – aridity between ~1550 cal yr BP and 600 cal yr BP

Enhanced aridity occurred right after the IRHP in the Padul peat bog area between ca. 1550 and 600 cal yr BP (ca. 400 - 1350 CE). This is deduced in the Padul-15-05 record by a significant forest decline, with a prominent decrease in Mediterranean forest, an increase in Cichorioideae herbs and the decline in the estimated water level (Unit 1; Pollen Zone 3; Figs. 4 and 7). A significant change since the end of the IRHP took place in the lake environment, suggesting the transition from a shallow water table to an ephemeral environment. This is deduced by the disappearance of charophytes, a significant decrease in Algae component and higher Si and MS and lower TOC values (Unit 1; Figs. 6 and 7).
This arid phase could be separated into two different periods. The first period occurred between ca. 1550 cal yr BP (ca. 400 CE) and ca. 1100 cal yr BP (ca. 900 CE) and is characterized by a decreasing trend in Mediterranean forest and *Botryococcus* taxa and the increase in Cichorioideae. This period corresponds with the Dark Ages [from ca. 500 to 900 CE; (Moreno et al., 2012)]. A visual correlation between the decrease in Mediterranean forest, the increase in the Drift Ice Index in the North Atlantic record (cold event 1; Bond et al., 2001), the decrease in SSTs in the Mediterranean Sea and maxima in positive NAO reconstructions suggests drier and colder conditions during this time (Fig. 6). Other Mediterranean and central-European records agree with our climate interpretations, for example, a decrease in forest extent is shown in a marine record from the Alboran Sea (Fletcher et al., 2013) and a decrease in lake levels is also observed in Central Europe (Magny et a., 2004) pointing to aridity during the DA. Evidences of aridity during the DA have been show too in the Mediterranean part of the Iberian Peninsula, for instance, cold and arid conditions were suggested in the northern Betic Range by the increase in

xerophytic herbs around 1450 and 750 cal yr BP (Carrión et al., 2001a) and in southeastern Spain by a forest decline in lacustrine deposits around 1620 and 1160 cal yr BP (Carrión et al., 2003). Arid and colder conditions during the Dark Ages (around 1680 to 1000 cal yr BP) are also suggested for the central part of the Iberian Peninsula using a multiproxy study of a sediment record from the Tablas de Daimiel Lake (Gil García et al., 2007).

A second period that we could differentiate within this overall arid phase occurred around 1100 to 600 cal yr BP/900 to 1350 CE, during the well-known MCA (900 to 1300 CE after Moreno et al., 2012). During this period the Padul-15-05 record shows a slight increasing trend in the Mediterranean forest taxa with respect to the DA, but the decrease in *Botryococcus* and the higher abundance of herbs still point to overall arid conditions. This change could be related to an increase in temperature, favoring the development of temperate forest species, and would agree with inferred increasing temperatures in the North Atlantic areas, as well as the increase in solar irradiance and the increase in SSTs in the Mediterranean Sea (Fig.7). This hypothesis would agree with the reconstruction of persistent positive NAO and overall warm conditions during the MCA in the western Mediterranean (see synthesis in Moreno et al., 2012). A similar pattern of increasing xerophytic vegetation during the MCA is observed in alpine peat bogs and lakes in the Sierra Nevada (Anderson et al., 2011; Jiménez-Moreno et al., 2013; Ramos-Román et al., 2016) and arid conditions are shown to occur during the MCA in southern and eastern Iberian Peninsula deduced by increases in salinity and lower lake levels (Corella et al., 2013; Martín-Puertas et al., 2011). However, humid conditions have been reconstructed for the northwestern of the Iberian Peninsula at this time (Lebreiro et al., 2006; Moreno et al., 2012), as well as northern Europe (Martín-Puertas et al., 2008). The different pattern of precipitation between the northwestern Iberian Peninsula / northern Europe and the Mediterranean area is undoubtedly a function of the well-known NAO dipole in precipitation pattern (Trouet et al., 2009).

5.2.4 The last ~600 cal yr BP: LIA (1350-1850 CE) and IE (1850 CE-Present)

Two climatically different periods can be distinguished during the last ca. 600 cal yr BP (end of Zone 3b to Zone 4; Fig. 4) in the area. However, the climatic signal is more difficult to interpret due to a higher human impact at that time. The first phase around 1350-1450 CE was characterized by increasing relative humidity by the decrease in xerophytes and the increase in Mediterranean forest taxa and *Botryococcus* after a period of decrease during the DA and MCA, corresponding to the LIA. The second phase is characterized here by the decrease in the Mediterranean forest around 1700-1850 CE, pointing to a return to more arid conditions during the last part of the LIA (Figs. 4 and 7). This climatic pattern agrees with an increase in precipitation by the transition from positive to negative NAO mode and from warmer to cooler conditions in the North Atlantic area during the first phase of the LIA and a second phase characterized by cooler (cold event 0; Bond et al., 2001) and drier conditions (Fig. 6). A stronger variability in the SSTs is described in the Mediterranean Sea during the LIA (Fig. 6). Mayewski et al. (2004) described a period of climate variability during the Holocene at this time (600 to 150 cal yr BP) suggesting a polar cooling but more humid in some parts of the tropics. Regionally, (Morellón et al., 2011) also described a phase of more humid conditions between 1530 to 1750 CE in a lake sediment record from NE Spain. An alternation between wetter to drier periods during the LIA are also shown in the nearby alpine record from Borreguil de la Caldera in the Sierra Nevada mountain range (Ramos-Román et al., 2016).

The environmental transition from ephemeral to emerged conditions, observed in the last ca. 1550 cal yr BP (Unit 1; Fig. 5), intensified in the last ca. 300 cal yr BP. This is shown by the highest MS and Si values the increase in wetland plants and the stronger decrease in Ca and organic components (TOC) in the sediments in the uppermost part of the Padul-15-05 record (Unit 2; Figs. 3 and 6).

5.3 Centennial-scale variability

Time series analysis has become important in determining the recurrent periodicity of cyclical oscillations in paleoenvironmental sequences (e.g. Jiménez-Espejo et al., 2014; Ramos-Román et al., 2016; Rodrigo-Gámiz et al., 2014; Fletcher et al., 2013). This analysis also assists in understanding possible relationships between the paleoenvironmental proxy data and the potential triggers of the observed cyclical changes: i.e., solar activity, atmospheric, oceanic dynamics and climate evolution during the Holocene. The cyclostratigraphic analysis on the pollen (Mediterranean forest; regional signal), algae (*Botryococcus*; local signal) and TOC (local signal) times series from the Padul-15-05 record evidence centennial-scale cyclical patterns with periodicities around 800, 680, 300, 240, 200 and 170 years above the 90 % confidence levels (Fig. 7).

Previous cyclostratigraphic analysis in Holocene western Mediterranean records suggest cyclical climatic oscillations with periodicities around 1500 and 1750 yr (Fletcher et al., 2013; Jiménez-Espejo et al., 2014; Rodrigo-Gámiz et al., 2014). Other North Atlantic and Mediterranean records also present cyclicities in their paleoclimatic proxies of ca. 1600 yr (Bond et al., 2001; Debret et al., 2007; Rodrigo-Gámiz et al., 2014). However, this cycle is absent from the cyclostratigraphic analysis in the Padul-15-05 record (Fig. 7). In contrast, the spectral analysis performed in the Mediterranean forest time series from Padul peat bog record, pointing to cyclical hydrological changes, shows a significant ~800 yr cycle that could be related to solar variability (Damon and Sonett, 1991) or could be the second harmonic of the ca. ~1600 yr oceanic-related cycle (Debret et al., 2009). A very similar periodicity of ca. 760 yr is detected in the *Pinus* forest taxa, also pointing to humidity variability, from the alpine Sierra Nevada site of Borreguil de la Caldera and seems to show that this is a common feature of cyclical paleoclimatic oscillation in the area.

A significant ~680 cycle is shown in the *Botryococcus* time series most likely suggesting recurrent centennial-scale changes in temperature (productivity) and water availability. A similar cycle is shown in the *Artemisia* signal in an alpine record from Sierra Nevada (Ramos-Román et al., 2016). This cycle around ~650 yr is also observed in a marine record from the Alboran Sea, and was interpreted as the secondary harmonic of the 1300 yr cycle that those authors related with cyclic thermohaline circulation and sea surface temperature changes (Rodrigo-Gámiz et al., 2014).

A statistically significant ~300 yr cycle is shown in the Mediterranean forest taxa and TOC from the Padul-15-05 record suggesting shorter-scale variability in water availability. This cycle is also observed in the cyclical *Pinus* pollen data from Borreguil de la Caldera at higher elevations in the Sierra Nevada (Ramos-Román et al., 2016). This cycle could be principally related to NAO variability as observed by Olsen et al. (2012), which follows variations in humidity observed in the Padul-15-05 record. NAO variability also regulates modern precipitation in the area.

The *Botryococcus* and TOC time series shows variability with a periodicity around ~240, 200 and 164 yrs. Sonnet et al. (1984) described a significant cycle in solar activity around ~208 yr

(Suess solar cycle), which could have triggered our ~200 cyclicity. The observed ~240 yr periodicity in the Padul-15-05 record could be either related to variations in solar activity or due to the mixed effect of the solar together with the ~300 yr NAO-interpreted cycle and could point to a solar origin of the centennial-scale NAO variations as suggested by previously published research (Lukianova and Alekseev, 2004; Zanchettin et al., 2008). Finally, a significant ~170 yr cycle has been observed in both the Mediterranean forest taxa and *Botryococcus* times series from the Padul-15-05 record. A similar cycle (between 168-174 yr) was also described in the alpine pollen record from Borreguil de la Caldera in Sierra Nevada (Ramos-Román et al., 2016), which shows that it is a significant cyclical pattern in climate, probably precipitation, in the area. This cycle could be related to the previously described ~170 yr cycle in the NAO index (Olsen et al., 2012), which would agree with the hypothesis of the NAO controlling millennial- and centennial-scale environmental variability during the Late Holocene in the area (García-Alix et al., 2017; Ramos-Román et al., 2016).

5.4 Human activity

Humans probably had an impact in the area since Prehistoric times, however, the Padul-15-05 multiproxy record shows a more significant human impact during the last ca. 1550 cal yr BP, which intensified in the last ca. 500 cal yr BP (since 1450 CE to Present). This is deduced by, a significant increase in nitrophilous plant taxa such as Cichorioideae, Convolvulaceae, Polygonaceae and *Plantago* and the increase in some NPP such as *Tilletia*, coprophilous fungi and thecamoebians (Unit 2; Pollen Zone 4; Fig. 4). Most of these pollen taxa and NPPs are described in other southern Iberian paleoenvironmental records as indicators of land uses, for instance, *Tilletia* and covarying Cichorioideae and Convolvulaceae have been described as indicators of farming (e.g. Carrión et al., 2001b). Interestingly, these taxa being to decline around ~1450 CE, coinciding with the higher increase in detritic material into the basin. Climatically, this event coincides with the start of persistent negative NAO conditions in the area (Trouet et al., 2009), which could have further triggered more rainfall and more detritic input into the basin. Bellin et al., 2011 in a study from the Betic Cordillera (southern Iberian Peninsula) demonstrate that soil erosion increase in years with higher rainfall and this could be intensified by human impact. Nevertheless, in a study in the southeastern part of the Iberian Peninsula (Bellin et al., 2013) suggested that major soil erosion could have occurred by the abandonment of agricultural activities in the mountain areas as well as the abandonment of irrigated terrace systems during the Christian Reconquest. Enhanced soil erosion at this time is also supported by the increase in *Glomus* type (Fig. 4).

An important change in the sedimentation in the environment is observed during the last ca. 300 cal yr BP marked by the stronger increase in MS and Si values. This was probably related with the Padul peat bog water drainage by humans using canals in the late XVIII century for cultivation purposes (Villegas Molina, 1967). The increase in wetland vegetation and higher values of Poaceae could be due to cultivation of cereals or by an increase in the population of *Phragmites australis* (also a Poaceae), very abundant in the Padul peat bog margins at present due to the increase in drained land surface.

The uppermost part (last ca. 100 cal yr BP) of the pollen record from Padul-15-05 shows an increasing trend in some arboreal taxa at that time, including Mediterranean forest, *Olea* and *Pinus* (Fig. 4). This change is most likely of human origin and generated by the increase in *Olea* cultivation in the last two centuries, also observed in many records from higher elevation sites from Sierra Nevada, and *Pinus* and other Mediterranean species reforestation in the 20th century

(Anderson et al., 2011; Jiménez-Moreno and Anderson, 2012; Jiménez-Moreno et al., 2013; Ramos-Román et al., 2016).

6 Conclusions

Our multiproxy (i.e. lithology, geochemistry, paleontology) analysis from the Padul-15-05 sequence has provided a detailed climate reconstruction for the last 4700 ca yr BP for the Padul peat bog area and the western Mediterranean. This study, supported by the comparison with other Mediterranean and North Atlantic records suggests a link between vegetation, atmospheric dynamics and insolation and solar activity during the Late Holocene in this area. A climatic aridification trend occurred during the Late Holocene in the Sierra Nevada and the western Mediterranean area, probably linked with the orbital-scale decreasing trend in summer insolation. This long-term trend is modulated by centennial-scale climate variability as shown by the pollen (Mediterranean forest taxa) algae (*Botryococcus*) and sedimentary and geochemical data in the Padul record. These events are in correlation with regional and global scale climate variability and cold and arid pulses around the 4200 and 3000 cal yr BP that are identified in this study seem to be synchronous with cold events recorded in the North Atlantic and decreases in precipitation in the Mediterranean area, probably linked to persistent positive NAO mode. Moreover, one of the most important humid and warmer periods during the Late Holocene in the Padul area coincides in time with the well-known IRHP, warm and humid conditions in the Mediterranean and North Atlantic regions and overall negative NAO conditions. A drastic decrease in Mediterranean forest taxa towards an open landscape, pointing to colder and enhanced aridity, occurred in two steps (DA and end of the LIA) during the last ca. 1550 cal yr BP. However, this trend was slightly superimposed by a more arid but warmer event coinciding with the MCA and a cold but wetter event during the first part of the LIA. Besides natural climatic and environmental variability, there seems to be intense human activities in the area during the last the last ca. 1550 cal yr BP. This suggests that the natural aridification trend during the Late Holocene in the western Mediterranean region could have been intensified due to the higher human activity in this area.

Furthermore, time series analyses done in the Padul-15-05 record show centennial-scale changes in the environment and climate that are coincident with the periodicities observed in solar, oceanic and NAO reconstructions and could show a close cause-and-effect linkage between them.

Acknowledgement

This work was supported by the project P11-RNM-7332 funded by Consejería de Economía, Innovación, Ciencia y Empleo de la Junta de Andalucía, the project CGL2013-47038-R funded by Ministerio de Economía y Competitividad of Spain and fondo Europeo de desarrollo regional FEDER and the research group RNM0190 (Junta de Andalucía). M. J. R.-R. acknowledges the PhD funding provided by Consejería de Economía, Innovación, Ciencia y Empleo de la Junta de Andalucía (P11-RNM-7332). J.C. acknowledges the PhD funding provided by Ministerio de Economía y Competitividad (CGL2013-47038-R). A.G.-A. was also supported by a Ramón y Cajal Fellowship RYC-2015-18966 of the Spanish Government (Ministerio de Economía y Competividad). Javier Jaimez (CIC-UGR) is thanked for graciously helping with the coring, the drilling equipment and logistics.

References

Abel-Schaad, D. and López-Sáez, J. A.: Vegetation changes in relation to fire history and human activities at the Peña Negra mire (Bejar Range, Iberian Central Mountain System, Spain) during the past 4,000 years, Veg. Hist. Archaeobotany, 22(3), 199–214, doi:10.1007/s00334-012-0368-9, 2013.

Al Aallali, A., Nieto, J. M. L., Raya, F. A. P. and Mesa, J. M.: Estudio de la vegetación forestal en la vertiente sur de Sierra Nevada (Alpujarra Alta granadina), Itinera Geobot., (11), 387–402, 1998.

Alfaro, P., Galinod-Zaldievar, J., Jabaloy, A., López-Garrido, A. C. and Sanz de Galdeano, C.: Evidence for the activity and paleoseismicity of the Padul fault (Betic Cordillera, Southern Spain) [Evidencias de actividad y paleosismicidad de la falla de Padul (Cordillera Bética, sur de España)], Acta Geol. Hisp., 36(3–4), 283–297, 2001.

Alpert, P., Baldi, M., Ilani, R., Krichak, S., Price, C., Rodó, X., Saaroni, H., Ziv, B., Kishcha, P., Barkan, J., Mariotti, A. and Xoplaki, E.: Chapter 2 Relations between climate variability in the Mediterranean region and the tropics: ENSO, South Asian and African monsoons, hurricanes and Saharan dust, Dev. Earth Environ. Sci., 4(C), 149–177, doi:10.1016/S1571-9197(06)80005-4, 2006.

Anderson, R. S., Jiménez-Moreno, G., Carrión, J. S. and Pérez-Martínez, C.: Postglacial history of alpine vegetation, fire, and climate from Laguna de Río Seco, Sierra Nevada, southern Spain, Quat. Sci. Rev., 30(13–14), 1615–1629, doi:https://doi.org/10.1016/j.quascirev.2011.03.005, 2011.

Bar-Matthews, M., Ayalon, A., Gilmour, M., Matthews, A. and Hawkesworth, C. J.: Sea–land oxygen isotopic relationships from planktonic foraminifera and speleothems in the Eastern Mediterranean region and their implication for paleorainfall during interglacial intervals, Geochim. Cosmochim. Acta, 67(17), 3181–3199, doi:https://doi.org/10.1016/S0016-7037(02)01031-1, 2003.

Bellin, N., Vanacker, V., van Wesemael, B., Solé-Benet, A. and Bakker, M. M.: Natural and anthropogenic controls on soil erosion in the internal betic Cordillera (southeast Spain), Catena, 87(2), 190–200, doi:10.1016/j.catena.2011.05.022, 2011.

Bellin, N., Vanacker, V. and De Baets, S.: Anthropogenic and climatic impact on Holocene sediment dynamics in SE Spain: A review, Quat. Int., 308–309, 112–129, doi:10.1016/j.quaint.2013.03.015, 2013.

Beug, H.-J.: Leitfaden der Pollenbestimmung für Mitteleuropa und angrenzende Gebiete, Fisch. Stuttg., 61, 1961.

Blaauw, M.: Methods and code for “classical” age-modelling of radiocarbon sequences, Quat. Geochronol., 5(5), 512–518, doi:https://doi.org/10.1016/j.quageo.2010.01.002, 2010.

727 Bond, G., Kromer, B., Beer, J., Muscheler, R., Evans, M. N., Showers, W., Hoffmann, S., Lotti-
728 Bond, R., Hajdas, I. and Bonani, G.: Persistent Solar Influence on North Atlantic Climate During
729 the Holocene, Science, 294(5549), 2130, doi:10.1126/science.1065680, 2001.

730 Booth, R. K., Jackson, S. T., Forman, S. L., Kutzbach, J. E., E. A. Bettis, I., Kreigs, J. and Wright, D.
731 K.: A severe centennial-scale drought in midcontinental North America 4200 years ago and
732 apparent global linkages, The Holocene, 15(3), 321–328, doi:10.1191/0959683605hl825ft,
733 2005.

734 Carrión, J. S.: Patterns and processes of Late Quaternary environmental change in a montane
735 region of southwestern Europe, Quat. Sci. Rev., 21(18–19), 2047–2066,
736 doi:https://doi.org/10.1016/S0277-3791(02)00010-0, 2002.

737 Carrión, J. S., Munuera, M., Dupré, M. and Andrade, A.: Abrupt vegetation changes in the
738 Segura Mountains of southern Spain throughout the Holocene, J. Ecol., 89(5), 783–797,
739 doi:10.1046/j.0022-0477.2001.00601.x, 2001a.

740 Carrión, J. S., Andrade, A., Bennett, K. D., Navarro, C. and Munuera, M.: Crossing forest
741 thresholds: inertia and collapse in a Holocene sequence from south-central Spain, The
742 Holocene, 11(6), 635–653, doi:10.1191/09596830195672, 2001b.

743 Carrión, J. S., Fernández, S., Jiménez-Moreno, G., Fauquette, S., Gil-Romera, G., González-
744 Sampériz, P. and Finlayson, C.: The historical origins of aridity and vegetation degradation in
745 southeastern Spain, J. Arid Environ., 74(7), 731–736,
746 doi:https://doi.org/10.1016/j.jaridenv.2008.11.014, 2010b.

747 Carrión, J. S., Sánchez-Gómez, P., Mota, J. F., Yll, R. and Chaín, C.: Holocene vegetation
748 dynamics, fire and grazing in the Sierra de Gádor, southern Spain, Holocene, 13(6), 839–849,
749 doi:10.1191/0959683603hl662rp, 2003.

750 Carrión, J. S., Fuentes, N., González-Sampériz, P., Quirante, L. S., Finlayson, J. C., Fernández, S.
751 and Andrade, A.: Holocene environmental change in a montane region of southern Europe with
752 a long history of human settlement, Quat. Sci. Rev., 26(11–12), 1455–1475,
753 doi:https://doi.org/10.1016/j.quascirev.2007.03.013, 2007.

754 Carrión, J. S., Fernández, S., González-Sampériz, P., Gil-Romera, G., Badal, E., Carrión-Marco, Y.,
755 López-Merino, L., López-Sáez, J. A., Fierro, E. and Burjachs, F.: Expected trends and surprises in
756 the Lateglacial and Holocene vegetation history of the Iberian Peninsula and Balearic Islands,
757 Rev. Palaeobot. Palynol., 162(3), 458–475,
758 doi:http://dx.doi.org/10.1016/j.revpalbo.2009.12.007, 2010.

759 Combourieu-Nebout, N., Peyron, O., Dormoy, I., Desprat, S., Beaudouin, C., Kotthoff, U. and
760 Marret, F.: Rapid climatic variability in the west Mediterranean during the last 25 000 years
761 from high resolution pollen data, Clim Past, 5(3), 503–521, doi:10.5194/cp-5-503-2009, 2009.

762 Corella, J. P., Stefanova, V., El Anjoumi, A., Rico, E., Giralt, S., Moreno, A., Plata-Montero, A. and

763 Valero-Garcés, B. L.: A 2500-year multi-proxy reconstruction of climate change and human
764 activities in northern Spain: The Lake Arreo record, Palaeogeogr. Palaeoclimatol. Palaeoecol.,
765 386, 555–568, doi:10.1016/j.palaeo.2013.06.022, 2013.

766 Currás, A., Zamora, L., Reed, J. M., García-Soto, E., Ferrero, S., Armengol, X., Mezquita-Joanes,
767 F., Marqués, M. A., Riera, S. and Julià, R.: Climate change and human impact in central Spain
768 during Roman times: High-resolution multi-proxy analysis of a tufa lake record (Somolinos,
769 1280m asl), Catena, 89(1), 31–53, doi:10.1016/j.catena.2011.09.009, 2012.

770 Damon, P. E. and Sonett, C. P.: Solar and terrestrial components of the atmospheric C-14
771 variation spectrum. In: Sonett, C.P., Giampapa, M.S., Matthews, M.S. (Eds.), The Sun in Time.
772 University of Arizona Press, Tucson, AZ, USA., 1991.

773 Debret, M., Bout-Roumazeilles, V., Grousset, F., Desmet, M., McManus, J. F., Massei, N., Sebag,
774 D., Petit, J.-R., Copard, Y. and Trentesaux, A.: The origin of the 1500-year climate cycles in
775 holocene north-atlantic records, Clim. Past, 3(4), 569–575, 2007.

776 Debret, M., Sebag, D., Crosta, X., Massei, N., Petit, J.-R., Chapron, E. and Bout-Roumazeilles, V.:
777 Evidence from wavelet analysis for a mid-Holocene transition in global climate forcing, Quat.
778 Sci. Rev., 28(25–26), 2675–2688, doi:https://doi.org/10.1016/j.quascirev.2009.06.005, 2009.

779 Delgado, J., Alfaro, P., Galindo-Zaldivar, J., Jabaloy, A., Lopez Garrido, A. and Sanz de Galdeano,
780 C.: Structure of the Padul-Nigüelas basin (S Spain) from H/V ratios of ambient noise: application
781 of the method to study peat and coarse sediments, Pure Appl. Geophys., 159(11), 2733–2749,
782 2002.

783 Domingo-García, M., Fernández-Rubio, R., Lopez, J. and González, C.: Aportación al
784 conocimiento de la Neotectónica de la Depresión del Padul (Granada), Tecniterrae, 53, 6–16,
785 1983.

786 Ejarque, A., Anderson, R. S., Simms, A. R. and Gentry, B. J.: Prehistoric fires and the shaping of
787 colonial transported landscapes in southern California: A paleoenvironmental study at Dune
788 Pond, Santa Barbara County, Quat. Sci. Rev., 112, 181–196,
789 doi:https://doi.org/10.1016/j.quascirev.2015.01.017, 2015.

790 Faegri, K. and Iversen, J.: Textbook of Pollen Analysis. Wiley, New York., 1989.

791 Fletcher, W. J. and Sánchez-Goñi, M. F.: Orbital- and sub-orbital-scale climate impacts on
792 vegetation of the western Mediterranean basin over the last 48,000 yr, Quat. Res., 70(3), 451–
793 464, doi:10.1016/j.yqres.2008.07.002, 2008.

794 Fletcher, W. J., Debret, M. and Sánchez-Goñi, M. F.: Mid-Holocene emergence of a low-
795 frequency millennial oscillation in western Mediterranean climate: Implications for past
796 dynamics of the North Atlantic atmospheric westerlies, The Holocene, 23(2), 153–166,
797 doi:10.1177/0959683612460783, 2013.

798 Florschütz, F., Amor, J. M. and Wijmstra, T. A.: Palynology of a thick quaternary succession in
799 southern Spain, Palaeogeogr. Palaeoclimatol. Palaeoecol., 10(4), 233–264,
800 doi:http://dx.doi.org/10.1016/0031-0182(71)90049-6, 1971.

801 García-Alix, A., Jimenez-Espejo, F. J., Lozano, J. A., Jiménez-Moreno, G., Martinez-Ruiz, F.,
802 Sanjuán, L. G., Jiménez, G. A., Alfonso, E. G., Ruiz-Puertas, G. and Anderson, R. S.:
803 Anthropogenic impact and lead pollution throughout the Holocene in Southern Iberia, Sci. Total
804 Environ., 449, 451–460, doi:https://doi.org/10.1016/j.scitotenv.2013.01.081, 2013.

805 García-Alix, A., Jiménez-Espejo, F. J., Toney, J. L., Jiménez-Moreno, G., Ramos-Román, M. J.,
806 Anderson, R. S., Ruano, P., Queralt, I., Delgado Huertas, A. and Kuroda, J.: Alpine bogs of
807 southern Spain show human-induced environmental change superimposed on long-term
808 natural variations, Sci. Rep., 7(1), 7439, doi:10.1038/s41598-017-07854-w, 2017.

809 van Geel, B., Hallewas, D. P. and Pals, J. P.: A late holocene deposit under the Westfriese Zeedijk
810 near Enkhuizen (Prov. of Noord-Holland, The Netherlands): Palaeoecological and archaeological
811 aspects, Rev. Palaeobot. Palynol., 38(3), 269–335, doi:http://dx.doi.org/10.1016/0034-
812 6667(83)90026-X, 1983.

813 van Geel, B., Coope, G. R. and Hammen, T. V. D.: Palaeoecology and stratigraphy of the
814 lateglacial type section at Usselo (the Netherlands), Rev. Palaeobot. Palynol., 60(1), 25–129,
815 doi:http://dx.doi.org/10.1016/0034-6667(89)90072-9, 1989.

816 Gil García, M. J., Ruiz Zapata, M. B., Santisteban, J. I., Mediavilla, R., López-Pamo, E. and Dabrio,
817 C. J.: Late holocene environments in Las Tablas de Daimiel (south central Iberian peninsula,
818 Spain), Veg. Hist. Archaeobotany, 16(4), 241–250, doi:10.1007/s00334-006-0047-9, 2007.

819 Gil-Romera, G., González-Sampériz, P., Lasheras-Álvarez, L., Sevilla-Callejo, M., Moreno, A.,
820 Valero-Garcés, B., López-Merino, L., Carrión, J. S., Pérez Sanz, A., Aranbarri, J. and García-Prieto
821 Fronce, E.: Biomass-modulated fire dynamics during the Last Glacial–Interglacial Transition at
822 the Central Pyrenees (Spain), Palaeogeogr. Palaeoclimatol. Palaeoecol., 402, 113–124,
823 doi:https://doi.org/10.1016/j.palaeo.2014.03.015, 2014.

824 Grimm, E. C.: CONISS: a FORTRAN 77 program for stratigraphically constrained cluster analysis
825 by the method of incremental sum of squares, Comput. Geosci., 13(1), 13–35,
826 doi:http://dx.doi.org/10.1016/0098-3004(87)90022-7, 1987.

827 Guy-Ohlson, D.: Botryococcus as an aid in the interpretation of palaeoenvironment and
828 depositional processes, Rev. Palaeobot. Palynol., 71(1), 1–15,
829 doi:http://dx.doi.org/10.1016/0034-6667(92)90155-A, 1992.

830 Hurrell, J. W.: Decadal Trends in the North Atlantic Oscillation: Regional Temperatures and
831 Precipitation, Science, 269(5224), 676, doi:10.1126/science.269.5224.676, 1995.

832 Jalut, G., Dedoubat, J. J., Fontugne, M. and Otto, T.: Holocene circum-Mediterranean vegetation
833 changes: Climate forcing and human impact, Quat. Int., 200(1–2), 4–18,

834 doi:https://doi.org/10.1016/j.quaint.2008.03.012, 2009.

835 Jiménez-Espejo, F. J., García-Alix, A., Jiménez-Moreno, G., Rodrigo-Gámiz, M., Anderson, R. S.,
836 Rodríguez-Tovar, F. J., Martínez-Ruiz, F., Giralt, S., Delgado Huertas, A. and Pardo-Igúzquiza, E.:
837 Saharan aeolian input and effective humidity variations over western Europe during the
838 Holocene from a high altitude record, Chem. Geol., 374–375, 1–12,
839 doi:10.1016/j.chemgeo.2014.03.001, 2014.

840 Jiménez-Moreno, G. and Anderson, R. S.: Holocene vegetation and climate change recorded in
841 alpine bog sediments from the Borreguiles de la Virgen, Sierra Nevada, southern Spain, Quat.
842 Res., 77(1), 44–53, doi:10.1016/j.yqres.2011.09.006, 2012.

843 Jiménez-Moreno, G., García-Alix, A., Hernández-Corbalán, M. D., Anderson, R. S. and Delgado-
844 Huertas, A.: Vegetation, fire, climate and human disturbance history in the southwestern
845 Mediterranean area during the late Holocene, Quat. Res., 79(2), 110–122,
846 doi:https://doi.org/10.1016/j.yqres.2012.11.008, 2013.

847 Jiménez-Moreno, G., Rodríguez-Ramírez, A., Pérez-Asensio, J. N., Carrión, J. S., López-Sáez, J. A.,
848 Villarías-Robles, J. J. R., Celestino-Pérez, S., Cerrillo-Cuenca, E., León, Á. and Contreras, C.:
849 Impact of late-Holocene aridification trend, climate variability and geodynamic control on the
850 environment from a coastal area in SW Spain, Holocene, 25(4), 607–617,
851 doi:10.1177/0959683614565955, 2015.

852 Kalugin, I., Daryin, A., Smolyaninova, L., Andreev, A., Diekmann, B. and Khlystov, O.: 800-yr-long
853 records of annual air temperature and precipitation over southern Siberia inferred from
854 Teletskoye Lake sediments, Quat. Res., 67(3), 400–410,
855 doi:https://doi.org/10.1016/j.yqres.2007.01.007, 2007.

856 Laskar, J., Robutel, P., Joutel, F., Gastineau, M., Correia, A. C. M. and Levrard, B.: A long-term
857 numerical solution for the insolation quantities of the Earth, A&A, 428(1), 261–285,
858 doi:10.1051/0004-6361:20041335, 2004.

859 Lebreiro, S. M., Francés, G., Abrantes, F. F. G., Diz, P., Bartels-Jónsdóttir, H. B., Stroynowski, Z.
860 N., Gil, I. M., Pena, L. D., Rodrigues, T., Jones, P. D., Nombela, M. A., Alejo, I., Briffa, K. R., Harris,
861 I. and Grimalt, J. O.: Climate change and coastal hydrographic response along the Atlantic
862 Iberian margin (Tagus Prodelta and Muros Ría) during the last two millennia, Holocene, 16(7),
863 1003–1015, doi:10.1177/0959683606hl990rp, 2006.

864 Lillios, K. T., Blanco-González, A., Drake, B. L. and López-Sáez, J. A.: Mid-late Holocene climate,
865 demography, and cultural dynamics in Iberia: A multi-proxy approach, Quat. Sci. Rev., 135, 138–
866 153, doi:https://doi.org/10.1016/j.quascirev.2016.01.011, 2016.

867 López-Sáez, J. A., Abel-Schaad, D., Pérez-Díaz, S., Blanco-González, A., Alba-Sánchez, F., Dorado,
868 M., Ruiz-Zapata, B., Gil-García, M. J., Gómez-González, C. and Franco-Múgica, F.: Vegetation
869 history, climate and human impact in the Spanish Central System over the last 9000 years,

870 Quat. Int., 353, 98–122, doi:https://doi.org/10.1016/j.quaint.2013.06.034, 2014.

871 Lukianova, R. and Alekseev, G.: Long-Term Correlation Between the Nao and Solar Activity, Sol.
872 Phys., 224(1), 445–454, doi:10.1007/s11207-005-4974-x, 2004.

873 Magny, M.: Holocene climate variability as reflected by mid-European lake-level fluctuations
874 and its probable impact on prehistoric human settlements, Quat. Int., 113(1), 65–79,
875 doi:https://doi.org/10.1016/S1040-6182(03)00080-6, 2004.

876 Magny, M., Peyron, O., Sadori, L., Ortu, E., Zanchetta, G., Vannière, B. and Tinner, W.:
877 Contrasting patterns of precipitation seasonality during the Holocene in the south- and north-
878 central Mediterranean, J. Quat. Sci., 27(3), 290–296, doi:10.1002/jqs.1543, 2012.

879 Magri, D.: Late Quaternary vegetation history at Lagaccione near Lago di Bolsena (central Italy),
880 Rev. Palaeobot. Palynol., 106(3–4), 171–208, doi:https://doi.org/10.1016/S0034-
881 6667(99)00006-8, 1999.

882 Marchal, O., Cacho, I., Stocker, T. F., Grimalt, J. O., Calvo, E., Martrat, B., Shackleton, N.,
883 Vautravers, M., Cortijo, E., Van Kreveld, S., Andersson, C., Koç, N., Chapman, M., Sbaffi, L.,
884 Duplessy, J.-C., Sarnthein, M., Turon, J.-L., Duprat, J. and Jansen, E.: Apparent long-term cooling
885 of the sea surface in the northeast Atlantic and Mediterranean during the Holocene, Quat. Sci.
886 Rev., 21(4–6), 455–483, doi:10.1016/S0277-3791(01)00105-6, 2002.

887 Martín-Puertas, C., Valero-Garcés, B. L., Mata, M. P., González-Sampériz, P., Bao, R., Moreno, A.
888 and Stefanova, V.: Arid and humid phases in southern Spain during the last 4000 years: the
889 Zoñar Lake record, Córdoba, The Holocene, 18(6), 907–921, doi:10.1177/0959683608093533,
890 2008.

891 Martín-Puertas, C., Valero-Garcés, B. L., Brauer, A., Mata, M. P., Delgado-Huertas, A. and Dulski,
892 P.: The Iberian-Roman Humid Period (2600-1600 cal yr BP) in the Zoñar Lake varve record
893 (Andalucía, southern Spain), Quat. Res., 71(2), 108–120, doi:10.1016/j.yqres.2008.10.004, 2009.

894 Martín-Puertas, C., Valero-Garcés, B. L., Mata, M. P., Moreno, A., Giralt, S., Martínez-Ruiz, F.
895 and Jiménez-Espejo, F.: Geochemical processes in a Mediterranean Lake: A high-resolution
896 study of the last 4,000 years in Zoñar Lake, southern Spain, J. Paleolimnol., 46(3), 405–421,
897 doi:10.1007/s10933-009-9373-0, 2011.

898 Mayewski, P. A., Rohling, E. E., Stager, J. C., Karlén, W., Maasch, K. A., Meeker, L. D., Meyerson,
899 E. A., Gasse, F., Kreveld, S. van, Holmgren, K., Lee-Thorp, J., Rosqvist, G., Rack, F., Staubwasser,
900 M., Schneider, R. R. and Steig, E. J.: Holocene climate variability, Quat. Res., 62(3), 243–255,
901 doi:https://doi.org/10.1016/j.yqres.2004.07.001, 2004.

902 Morellón, M., Valero-Garcés, B., Vegas-Vilarrúbia, T., González-Sampériz, P., Romero, Ó.,
903 Delgado-Huertas, A., Mata, P., Moreno, A., Rico, M. and Corella, J. P.: Lateglacial and Holocene
904 palaeohydrology in the western Mediterranean region: The Lake Estanya record (NE Spain),
905 Quat. Sci. Rev., 28(25–26), 2582–2599, doi:https://doi.org/10.1016/j.quascirev.2009.05.014,

2009.

Morellón, M., Valero-Garcés, B., González-Sampériz, P., Vegas-Vilarrúbia, T., Rubio, E., Rieradevall, M., Delgado-Huertas, A., Mata, P., Romero, Ó., Engstrom, D. R., López-Vicente, M., Navas, A. and Soto, J.: Climate changes and human activities recorded in the sediments of Lake Estanya (NE Spain) during the Medieval Warm Period and Little Ice Age, J. Paleolimnol., 46(3), 423–452, doi:10.1007/s10933-009-9346-3, 2011.

Moreno, A., Cacho, I., Canals, M., Grimalt, J. O., Sánchez-Goñi, M. F., Shackleton, N. and Sierro, F. J.: Links between marine and atmospheric processes oscillating on a millennial time-scale. A multi-proxy study of the last 50,000 yr from the Alboran Sea (Western Mediterranean Sea), Quat. Sci. Rev., 24(14–15), 1623–1636, doi:https://doi.org/10.1016/j.quascirev.2004.06.018, 2005.

Moreno, A., Pérez, A., Frigola, J., Nieto-Moreno, V., Rodrigo-Gámiz, M., Martrat, B., González-Sampériz, P., Morellón, M., Martín-Puertas, C., Corella, J. P., Belmonte, Á., Sancho, C., Cacho, I., Herrera, G., Canals, M., Grimalt, J. O., Jiménez-Espejo, F., Martínez-Ruiz, F., Vegas-Vilarrúbia, T. and Valero-Garcés, B. L.: The Medieval Climate Anomaly in the Iberian Peninsula reconstructed from marine and lake records, Quat. Sci. Rev., 43, 16–32, doi:https://doi.org/10.1016/j.quascirev.2012.04.007, 2012.

Nestares, T. and Torres, T. de: Un nuevo sondeo de investigación paleoambiental del Pleistoceno y Holoceno en la turbera del Padul (Granada, Andalucía). Geogaceta 23, 99-102., 1997.

Olsen, J., Anderson, N. J. and Knudsen, M. F.: Variability of the North Atlantic Oscillation over the past 5,200 years, Nat. Geosci, 5(11), 808–812, doi:10.1038/ngeo1589, 2012.

Ortiz, J. E., Torres, T., Delgado, A., Julià, R., Lucini, M., Llamas, F. J., Reyes, E., Soler, V. and Valle, M.: The palaeoenvironmental and palaeohydrological evolution of Padul Peat Bog (Granada, Spain) over one million years, from elemental, isotopic and molecular organic geochemical proxies, Org. Geochem., 35(11–12), 1243–1260, doi:https://doi.org/10.1016/j.orggeochem.2004.05.013, 2004.

Paillard, D., Labeyrie, L. and Yiou, P.: Macintosh Program performs time-series analysis, Eos Trans. Am. Geophys. Union, 77(39), 379–379, doi:10.1029/96EO00259, 1996.

Pérez Raya, F. and López Nieto, J.: Vegetación acuática y helofítica de la depresión de Padul (Granada), Acta Bot Malacit., 16(2), 373–389, 1991.

Pons, A. and Reille, M.: The holocene- and upper pleistocene pollen record from Padul (Granada, Spain): A new study, Palaeogeogr. Palaeoclimatol. Palaeoecol., 66(3), 243–263, doi:http://dx.doi.org/10.1016/0031-0182(88)90202-7, 1988.

Ramos-Román, M. J., Jiménez-Moreno, G., Anderson, R. S., García-Alix, A., Toney, J. L., Jiménez-Espejo, F. J. and Carrión, J. S.: Centennial-scale vegetation and North Atlantic Oscillation

changes during the Late Holocene in the southern Iberia, Quat. Sci. Rev., 143, 84–95, doi:https://doi.org/10.1016/j.quascirev.2016.05.007, 2016.

Reimer, P. J., Bard, E., Bayliss, A., Beck, J. W., Blackwell, P. G., Ramsey, C. B., Buck, C. E., Cheng, H., Edwards, R. L., Friedrich, M., Grootes, P. M., Guilderson, T. P., Haflidason, H., Hajdas, I., Hatté, C., Heaton, T. J., Hoffmann, D. L., Hogg, A. G., Hughen, K. A., Kaiser, K. F., Kromer, B., Manning, S. W., Niu, M., Reimer, R. W., Richards, D. A., Scott, E. M., Southon, J. R., Staff, R. A., Turney, C. S. M. and van der Plicht, J.: IntCal13 and Marine13 Radiocarbon Age Calibration Curves 0–50,000 Years cal BP, Radiocarbon, 55(4), 1869–1887, doi:10.2458/azu_js_rc.55.16947, 2013.

Riera, S., Wansard, G. and Julià, R.: 2000-year environmental history of a karstic lake in the Mediterranean Pre-Pyrenees: the Estanya lakes (Spain), {CATENA}, 55(3), 293–324, doi:https://doi.org/10.1016/S0341-8162(03)00107-3, 2004.

Riera, S., López-Sáez, J. A. and Julià, R.: Lake responses to historical land use changes in northern Spain: The contribution of non-pollen palynomorphs in a multiproxy study, Rev. Palaeobot. Palynol., 141(1–2), 127–137, doi:https://doi.org/10.1016/j.revpalbo.2006.03.014, 2006.

Rodrigo-Gámiz, M., Martínez-Ruiz, F., Rodríguez-Tovar, F. J., Jiménez-Espejo, F. J. and Pardo-Igúzquiza, E.: Millennial- to centennial-scale climate periodicities and forcing mechanisms in the westernmost Mediterranean for the past 20,000 yr, Quat. Res., 81(1), 78–93, doi:https://doi.org/10.1016/j.yqres.2013.10.009, 2014.

Sanz de Galdeano, C., El Hamdouni, R. and Chacón, J.: Neotectónica de la fosa del Padul y del Valle de Lecrín, Itiner. Geomorfológicos Por Andal. Orient. Publicacions Univ. Barc. Barc., 65–81, 1998.

Schulz, M. and Mudelsee, M.: REDFIT: estimating red-noise spectra directly from unevenly spaced paleoclimatic time series, Comput. Geosci., 28(3), 421–426, doi:https://doi.org/10.1016/S0098-3004(01)00044-9, 2002.

Sicre, M.-A., Jalali, B., Martrat, B., Schmidt, S., Bassetti, M.-A. and Kallel, N.: Sea surface temperature variability in the North Western Mediterranean Sea (Gulf of Lion) during the Common Era, Earth Planet. Sci. Lett., 456, 124–133, doi:http://dx.doi.org/10.1016/j.epsl.2016.09.032, 2016.

Steinhilber, F., Beer, J. and Fröhlich, C.: Total solar irradiance during the Holocene, Geophys. Res. Lett., 36(19), n/a–n/a, doi:10.1029/2009GL040142, 2009.

Trouet, V., Esper, J., Graham, N. E., Baker, A., Scourse, J. D. and Frank, D. C.: Persistent Positive North Atlantic Oscillation Mode Dominated the Medieval Climate Anomaly, Science, 324(5923), 78, doi:10.1126/science.1166349, 2009.

Valle, F.: Mapa de series de vegetación de Andalucía 1: 400 000, Editorial Rueda., 2003.

978 Villegas Molina, F.: Laguna de Padul: Evolución geológico-histórica, Estud. Geográficos, 28(109),
979 561, 1967.

980 Zanchettin, D., Rubino, A., Traverso, P. and Tomasino, M.: Impact of variations in solar activity
981 on hydrological decadal patterns in northern Italy, J. Geophys. Res. Atmospheres, 113(D12),
982 n/a–n/a, doi:10.1029/2007JD009157, 2008.

983
984
985
986
987
988
989
990
991
992
993
994
995
996
997
998
999
1000
1001
1002
1003
1004

Clim. Past Discuss., https://doi.org/10.5194/cp-2017-104
Manuscript under review for journal Clim. Past
Discussion started: 24 August 2017

Climate of the Past Discussions
Open Access
EGU

1005 **Figures and tables**

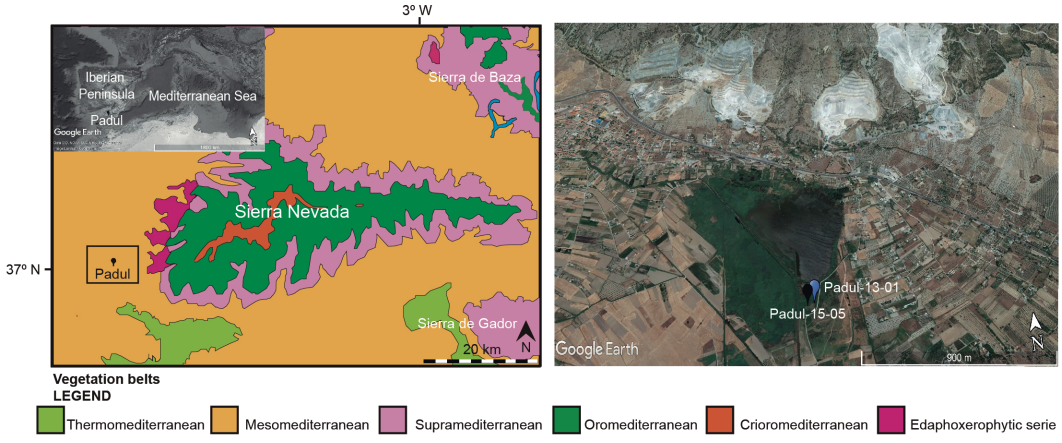

1006

1007 **Figure 1.** Location of Padul peat bog in Sierra Nevada National Park, southern Iberian
1008 Peninsula. Panel on the left is the map of the vegetation belts in the Sierra Nevada (Modified
1009 from REDIAM. Map of the vegetation series of Andalusia:
1010 http://laboratorioredIAM.cica.es/VisorGenerico/?tipo=WMS&url=http://www.juntadeandalucia.e
1011 s/medioambiente/mapwms/REDIAM_Series_Vegetacion_Andalucia?). The inset map is the
1012 Google earth image of the Iberian Peninsula in the Mediterranean region. Panel on the right is
1013 the Google earth image (http://www.google.com/earth/index.html) of Padul peat bog area
1014 showing the coring locations.

1015

1016

Clim. Past Discuss., https://doi.org/10.5194/cp-2017-104
Manuscript under review for journal Clim. Past
Discussion started: 24 August 2017

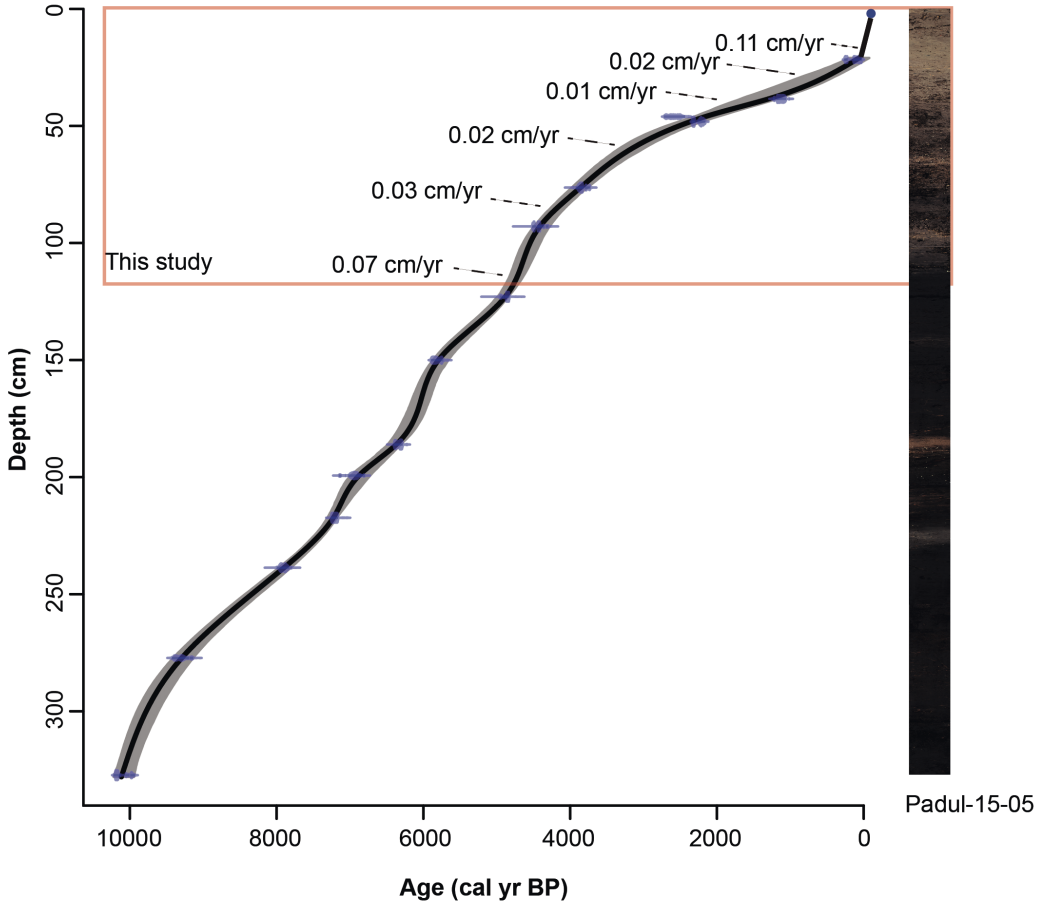

1017

1018 **Figure 2.** Photo of the Padul-15-05 sediment core with the age-depth model showing the part of
1019 the record that was studied here (red rectangle). The sediment accumulation rates (SAR) between
1020 individual segments are marked. See the body of the text for the explanation of the age
1021 reconstructions.

1022

1023

Clim. Past Discuss., https://doi.org/10.5194/cp-2017-104
Manuscript under review for journal Clim. Past
Discussion started: 24 August 2017

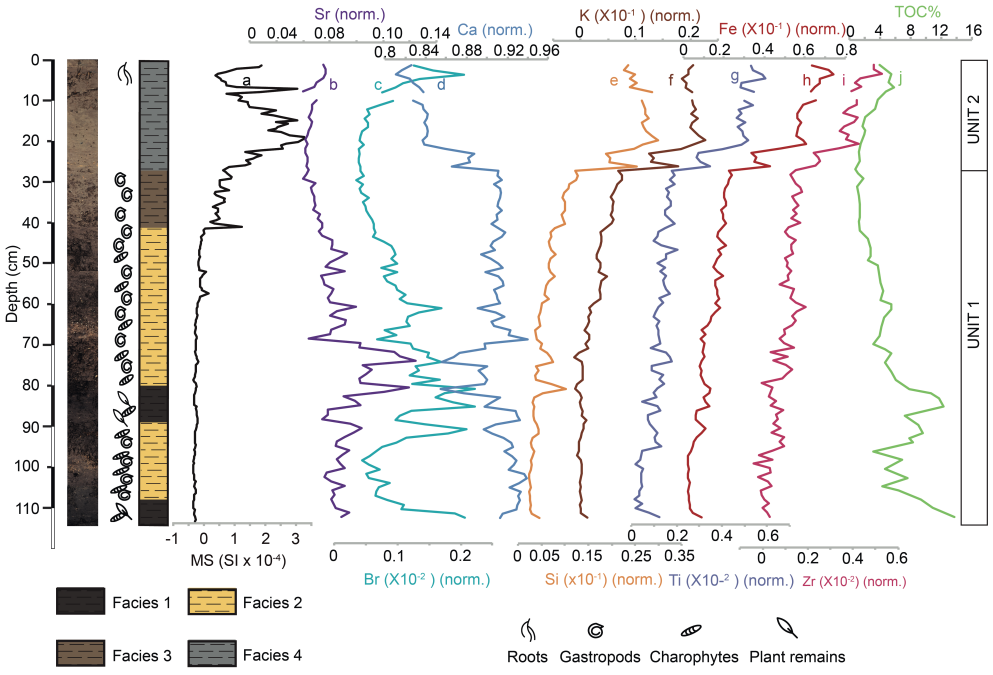

Figure 3. Lithology, facies interpretation with paleontology, magnetic susceptibility (MS), and geochemical (X-ray fluorescence (XRF) and total organic carbon (TOC) data from the Padul-15-05 record. XRF elements are represented normalized by the total counts. (a) Magnetic susceptibility (MS; SI). (b) Strontium normalized (Sr; norm.). (c) Bromine norm. (Br; norm.). (d) Calcium normalized. (Ca; norm.). (e) Silica normalized (Si; norm.). (f) Potassium normalized (K; norm.). (g) Titanium normalized (Ti; norm.). (h) Iron normalized (Fe; norm.). (i) Zirconium normalized (Zr; norm.). (j) Total organic carbon (TOC %).

Clim. Past Discuss., https://doi.org/10.5194/cp-2017-104
Manuscript under review for journal Clim. Past
Discussion started: 24 August 2017

Climate of the Past
Discussions
Open Access
EGU

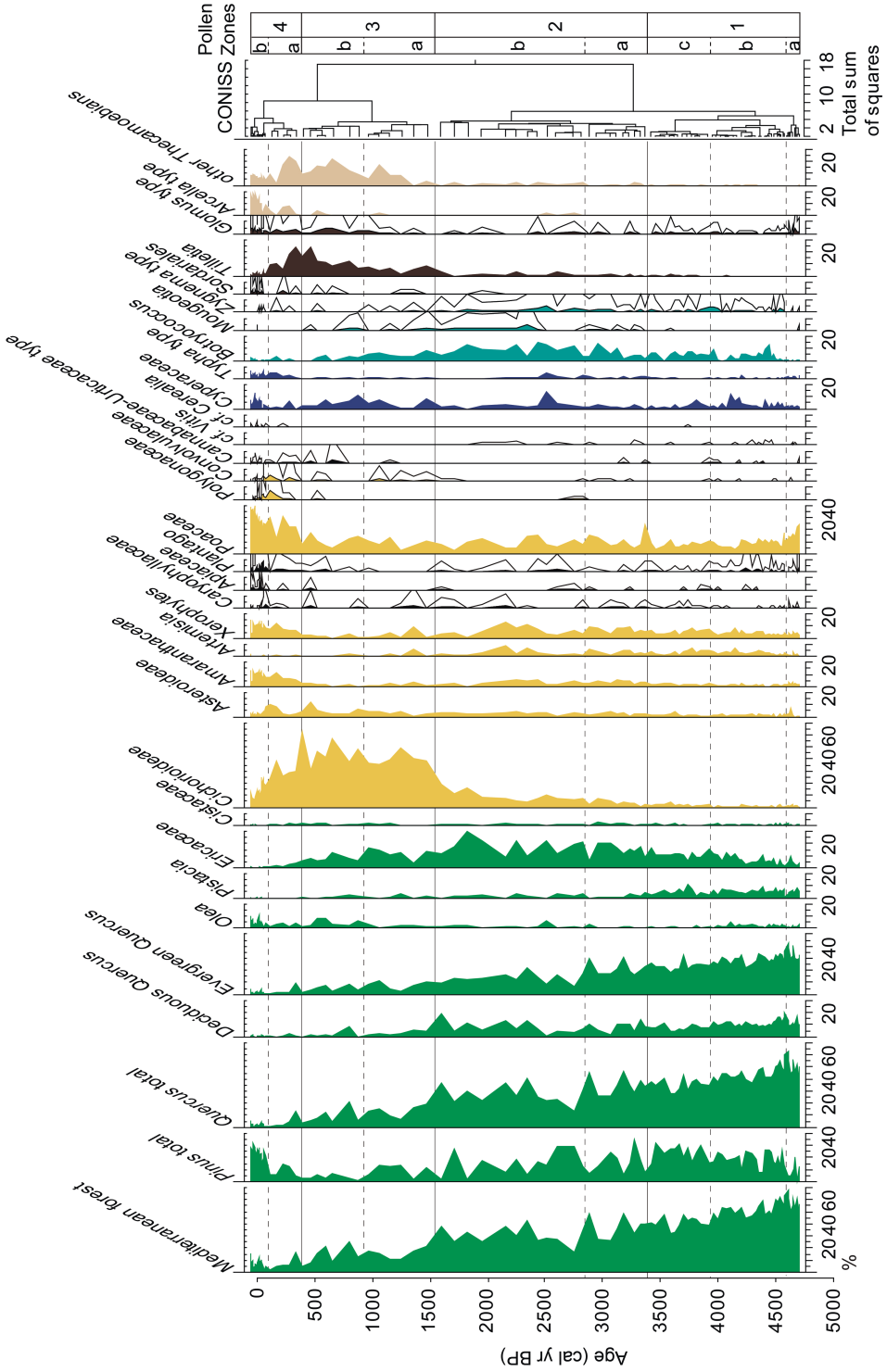

Clim. Past Discuss., https://doi.org/10.5194/cp-2017-104
Manuscript under review for journal Clim. Past
Discussion started: 24 August 2017

Climate of the Past Discussions
Open Access
EGU

Figure 4. Percentages of selected pollen taxa and non-pollen palynomorphs (NPPs) from the Padul-15-05 record, represented with respect to terrestrial pollen sum. Silhouettes show 7-time exaggerations of pollen percentages. Pollen zonation is shown on the right. Tree and shrubs are showing in green, herbs and grasses in yellow, aquatics in dark blue, algae in blue, fungi in brown and thecamoebians in beige. The Mediterranean forest taxa is composed of *Quercus* total, *Olea*, *Phillyrea* and *Pistacia*. The xerophyte group includes *Artemisia*, *Ephedra*, and Amaranthaceae.

Clim. Past Discuss., https://doi.org/10.5194/cp-2017-104
Manuscript under review for journal Clim. Past
Discussion started: 24 August 2017

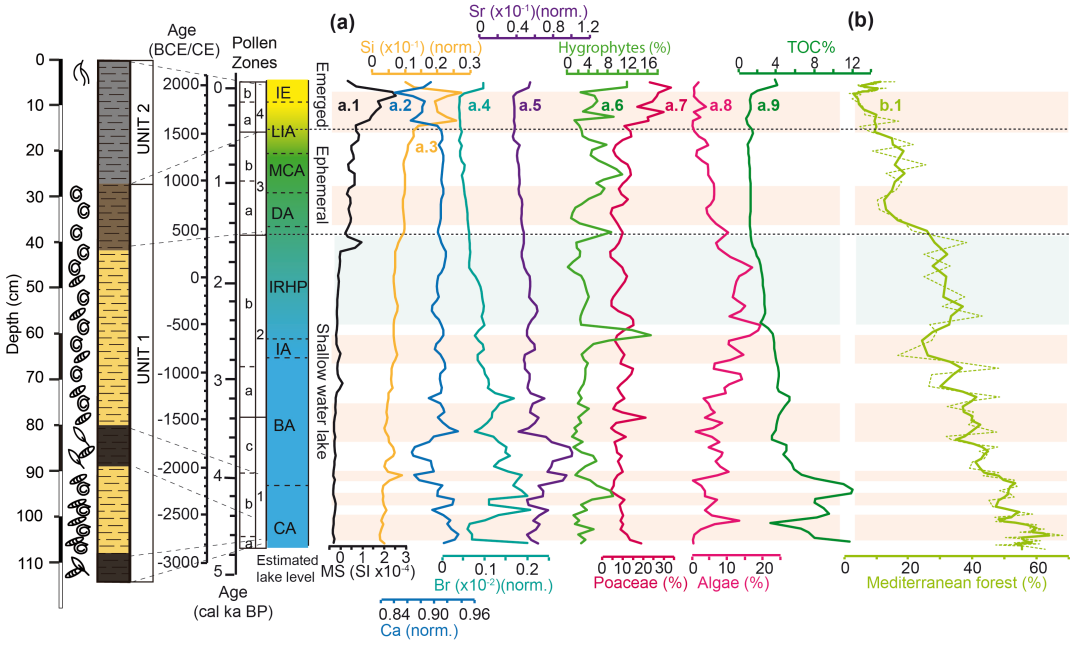

Figure 5. Estimated lake level evolution and regional palynological component from the last ca. 4700 yr based on the synthesis of determinate proxies from the Padul-15-05 record: (a) Proxies used to estimate the water table evolution from the Padul-15-05 record (proxies were resampled at 50 yr (lineal interpolation) using Past software http://palaeo-electronica.org/2001_1/past/issue1_01.htm). [(a.1) Magnetic Susceptibility (MS) in SI; (a.2) Silica normalized (Si; norm.); (a.3) Calcium normalized (Ca; norm.); (a.4) Bromine normalized (Br; norm.) ; (a.5) Strontium normalized (Sr; norm.); (a.6) Hygrophytes (%); (a.7) Poaceae (%); (a.8) Algae (%) (a.9) Total organic carbon (TOC %)] (b) Mediterranean forest taxa, with a smoothing of three-point in bold. Pink and blue shading indicates Holocene arid and humid regionally events, respectively. See the body of the text for the explanation of the lake level reconstruction. Mediterranean forest smoothing was made using Analyseries software (Paillard et al., 1996). CA = Copper Age; BA = Bronze Age; IA = Iron Age; IRHP = Iberian Roman Humid Period; DA = Dark Ages; MCA = Medieval Climate Anomaly; LIA = Little Ice Age; IE = Industrial Era.

Clim. Past Discuss., https://doi.org/10.5194/cp-2017-104
Manuscript under review for journal Clim. Past
Discussion started: 24 August 2017

Climate of the Past Discussions
Open Access
EGU

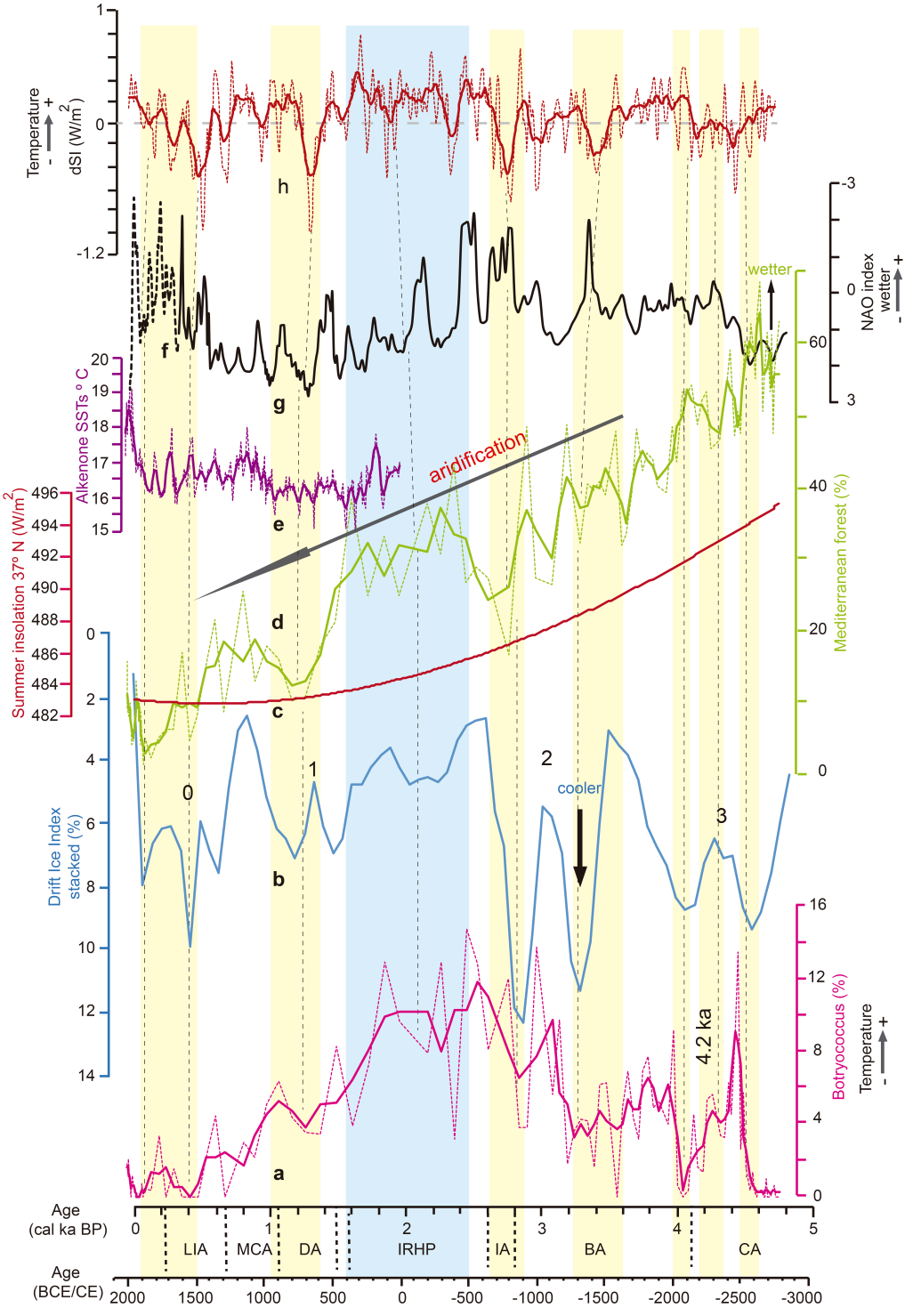

Clim. Past Discuss., https://doi.org/10.5194/cp-2017-104
Manuscript under review for journal Clim. Past
Discussion started: 24 August 2017

Climate of the Past Discussions
Open Access
EGU

1075 **Figure 6.** Comparison of the last ca. 4700 yr between different pollen taxa from the Padul-15-05
1076 record, summer insolation for the Sierra Nevada latitude, eastern Mediterranean humidity and
1077 North Atlantic temperature. (a) *Botryococcus* from the Padul-15-05 record, with a smoothing of
1078 three-point in bold (this study). (b) Drift Ice Index (reversed) from the North Atlantic (Bond et
1079 al., 2001). (c) Summer insolation calculated for 37º N (Laskar et al., 2004). (d) Mediterranean
1080 forest taxa from the Padul-15-05 record, with a smoothing of three-point in bold (this study). (e)
1081 Alkenone-SSTs from the Gulf of Lion (Sicre et al., 2016), with a smoothing of four-point in
1082 bold. (f) North Atlantic Oscillation (NAO) index from a climate proxy reconstruction from
1083 Morocco and Scotland (Trouet et al., 2009). (g) North Atlantic Oscillation (NAO) index
1084 (reversed) from a climate proxy reconstruction from Greenland (Olsen et al., 2012). (h) Total
1085 solar irradiance reconstruction from cosmogenic radionuclide from a Greenland ice core
1086 (Steinhilber et al., 2009), with a smoothing of twenty-one-point in bold. Yellow and blue shading
1087 correspond with arid (and cold) and humid (and warm) periods, respectively. Grey dash lines
1088 show a tentative correlation between arid and cold conditions and the decrease in the
1089 Mediterranean forest and *Botryococcus*. Mediterranean forest, *Botryococcus* and solar irradiance
1090 smoothing was made using Analyseries software (Paillard et al., 1996), Alkenone-SSTs
1091 smoothing was made using Past software (http://palaeo-
1092 electronica.org/2001_1/past/issue1_01.htm). A linear r (Pearson) correlation was calculated
1093 between *Botryococcus* (detrended) and Drift Ice Index (Bond et al., 2001; r = -0.63; $p < 0.0001$;
1094 between ca. 4700 to 1500 cal ka BP – r=-0.48; $p < 0.0001$ between 4700 and -65 cal yr BP).
1095 Previously, the data were detrended (only in *Botryococcus*), resampled at 70-yr (linear
1096 interpolation) in order to obtain equally spaced time series and smoothed to three-point average.
1097 CA = Copper Age; BA = Bronze Age; IA = Iron Age; IRHP = Iberian Roman Humid Period;
1098 DA = Dark Ages; MCA = Medieval Climate Anomaly; LIA = Little Ice Age; IE = Industrial Era.

1099

1100

1101

1102

1103

1104

1105

1106

Clim. Past Discuss., https://doi.org/10.5194/cp-2017-104
Manuscript under review for journal Clim. Past
Discussion started: 24 August 2017

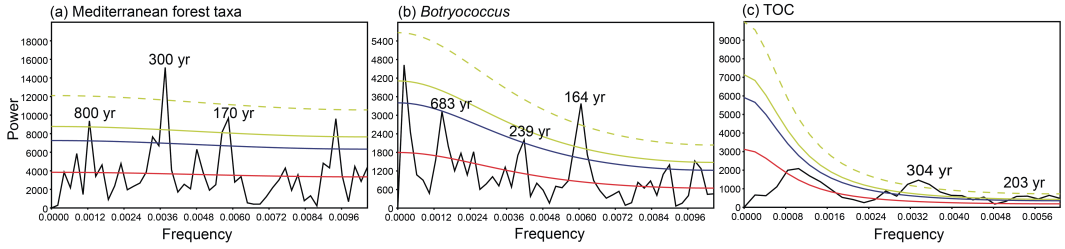

Figure 7. Spectral analysis of (a) Mediterranean forest taxa and (b) *Botryococcus* (mean sampling space = 47 yr) and (c) TOC (mean sampling space = 78 yr) from the Padul-15-05. The significant periodicities above confident level are shown. Confidence level 90 % (blue line), 95 % (green line), 99 % (green dash line) and AR (1) red noise (red line). Spectral analysis was made with Past software (http://palaeo- electronica.org/2001_1/past/issue1_01.htm).

Clim. Past Discuss., https://doi.org/10.5194/cp-2017-104
Manuscript under review for journal Clim. Past
Discussion started: 24 August 2017

Climate of the Past Discussions
Open Access
EGU

Table 1. Age data for Padul-15-05 record. All ages were calibrated using R-code package 'clam 2.2' employing the calibration curve IntelCal 13 (Reimer et al., 2013) at 95 % of confident range.

*Sample number assigned at radiocarbon laboratory

Laboratory number	Core	Material	Depth (cm)	Age (^{14}C yr BP ± 1σ)	Calibrated age (cal yr BP) 95 % confidence interval	Median age (cal yr BP)
Reference ages			0	2015CE	-65	-65
D-AMS 008531	Padul-13-01	Plant remains	21.67	103 ± 24	23-264	127
Poz-77568	Padul-15-05	Org. bulk sed.	38.46	1205 ± 30	1014-1239	1130
BETA-437233	Padul-15-05	Plant remains	46.04	2480 ± 30	2385-2722	2577
Poz-77569	Padul-15-05	Org. bulk sed.	48.21	2255 ± 30	2158-2344	2251
BETA-415830	Padul-15-05	Shell	71.36	3910 ± 30	4248-4421	4343
BETA-437234	Padul-15-05	Plant remains	76.34	3550 ± 30	3722-3956	3838
BETA-415831	Padul-15-05	Org. bulk sed.	92.94	3960 ± 30	4297-4519	4431
Poz-74344	Padul-15-05	Plant remains	122.96	4295 ± 35	4827-4959	4871
BETA-415832	Padul-15-05	Plant remains	150.04	5050 ± 30	5728-5900	5814
Poz-77571	Padul-15-05	Plant remains	186.08	5530 ± 40	6281-6402	6341
Poz-74345	Padul-15-05	Plant remains	199.33	6080 ± 40	6797-7154	6935
BETA-415833	Padul-15-05	Org. bulk sed.	217.36	6270 ± 30	7162-7262	7212
Poz-77572	Padul-15-05	Org. bulk sed.	238.68	7080 ± 50	7797-7999	7910
Poz-74347	Padul-15-05	Plant remains	277.24	8290 ± 40	9138-9426	9293
BETA-415834	Padul-15-05	Plant remains	327.29	8960 ± 30	9932-10221	10107

Clim. Past Discuss., https://doi.org/10.5194/cp-2017-104
Manuscript under review for journal Clim. Past
Discussion started: 24 August 2017

Climate of the Past Discussions
Open Access
EGU

1137 **Table 2.** Linear r (Pearson) correlation between geochemical elements from the Padul-15-05
1138 record. Statistical treatment was performed using the Past software (http://palaeo-
1139 electronica.org/2001_1/past/issue1_01.htm).

1140

	Si	K	Ca	Ti	Fe	Zr	Br	Sr
Si		8.30E-80	2.87E-34	7.47E-60	3.22E-60	5.29E-44	0.001152	7.79E-09
K	0.98612		7.07E-29	6.05E-60	8.20E-68	1.77E-51	0.00030317	5.38E-12
Ca	-0.88096	-0.84453		6.09E-42	5.81E-39	8.10E-34	0.35819	0.26613
Ti	0.96486	0.96501	-0.91794		1.74E-74	1.12E-57	0.074223	8.88E-07
Fe	0.96546	0.97577	-0.90527	0.98224		2.77E-66	0.051072	3.32E-08
Zr	0.92566	0.94789	-0.8783	0.96109	0.97398		0.054274	7.16E-08
Br	-0.31739	-0.3506	-0.091917	-0.17755	-0.19372	-0.19116		4.03E-18
Sr	-0.53347	-0.61629	0.11113	-0.46426	-0.51386	-0.50295	0.72852	

1141

1142

1143

1144

1145

1146

1147

1148

1149

1150

1151

1152

1153

1154

1155

1156

1157